Chapter 2: Literature review

As this is another study on ilmenite roasting I review the current body of knowledge in chapter 2. The scholarship review is organized according to:

2.1 TiO_2 pigment and titanium containing feed material industries
2.2 Exploitation of heavy minerals resources
2.3 Definition of crude ilmenite and its constituents
2.4 Beneficiation of crude ilmenite from Southern African East Coast deposits
2.5 Description of alternative flow lines to beneficiate crude ilmenite from Southern African East Coast deposits
2.6 Describing the principles of magnetic beneficiation
2.7 Descriptions of the principles of magnetization
2.8 Magnetic susceptibility of chromite
2.9 Mechanism of magnetic susceptibility changes in ilmenite
2.10 Defining roasting
2.11 Phase chemical changes during oxidative roasting
2.12 Equipment
2.13 Findings and conclusions

Magnetism, the mechanism of changes in magnetic susceptibility of ilmenite and the enhancement of magnetic susceptibility of ilmenite by roasting in an oxidative atmosphere are discussed in detail. The other scholarships (TiO_2 industry; exploitation of heavy minerals resources; definition of crude ilmenite and its constituents; beneficiation of Southern African East Cost deposits and equipment) are touched on either to clarify concepts or for comprehensiveness. The chapter is concluded with a discussion on how the test program followed in the study was derived from this scholarship review.

2.1 Discussion of the TiO_2 pigment and titanium containing feed material industries

Fisher (1997) gave an excellent review on the history of titanium dioxide consumption, from discovering its use as a pigment in 1908 to its current status as the white pigment used as opacifier in paints, paper and fibres and a variety of other end uses. Being more environmental friendly it replaced competing white lead pigments in the 1950s and 1960s. Considered a 'quality of life' product, the overall level of economic activity on a national and international level governs the consumption of the TiO_2 pigment. Consumption has been rising since the 1950s (figure 2.1 after Fisher 1997).

Figure 2.2 is an overview of the link between the TiO_2 pigment industry and the titanium-containing feed materials industry. Two commercial processes are utilized to produce titanium dioxide pigments. These are the sulphate process and the chloride process – the former being the older of the two processes. The chloride process is replacing the sulphate process due to commercial and environmental improvements. In 1997 57 per cent of all TiO_2 pigment was produced via the chloride process (Fisher 1997).

The sulphate process is a batch process with the following sequential primary unit operations (Fisher 1997):
1. Digestion where the TiO_2 containing feed material reacts with sulphuric acid to produce titanyl sulphate.
2. Precipitation of titanium dioxide hydrate.
3. Separation and washing of the hydrate.
4. Calcination and thermal formation of the pure TiO_2 crystals.

The chloride process is a continuous process with the following sequential primary unit operations (Fisher 1997):
1. Chlorination where chlorine reacts with the titanium containing feed materials under reducing conditions, at elevated temperature.
2. Condensation and purification where the low, medium and high boiling point chlorides are separated by fractional distillation.
3. Oxidation of the titanium tetrachloride with oxygen at elevated temperatures to form titanium dioxide pigment particles.

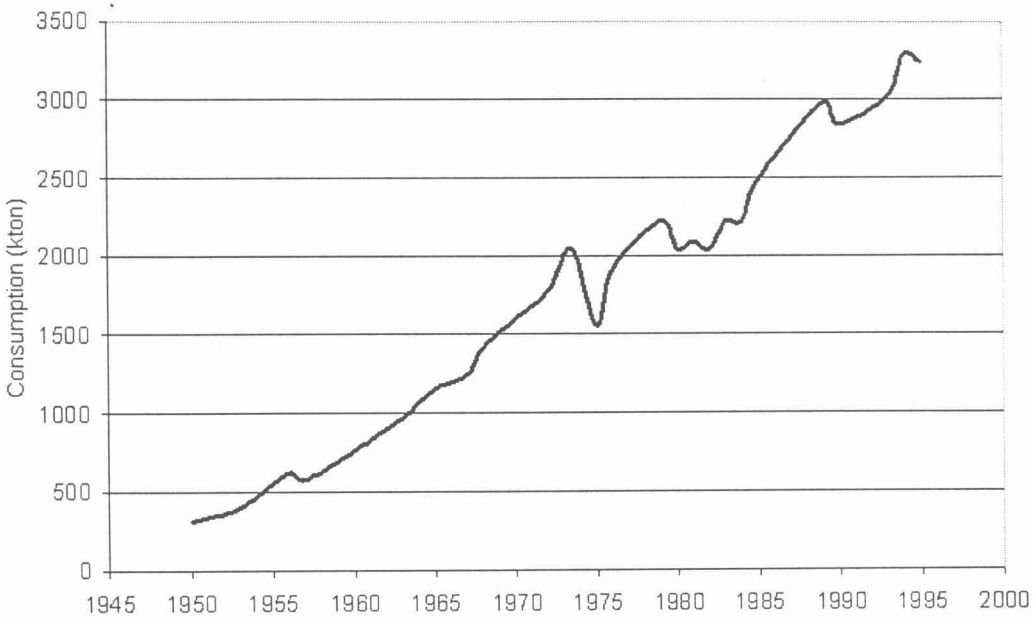

Figure 2.1: Worldwide TiO_2 pigment consumption from 1950 to 1995 - after Fisher (1997).

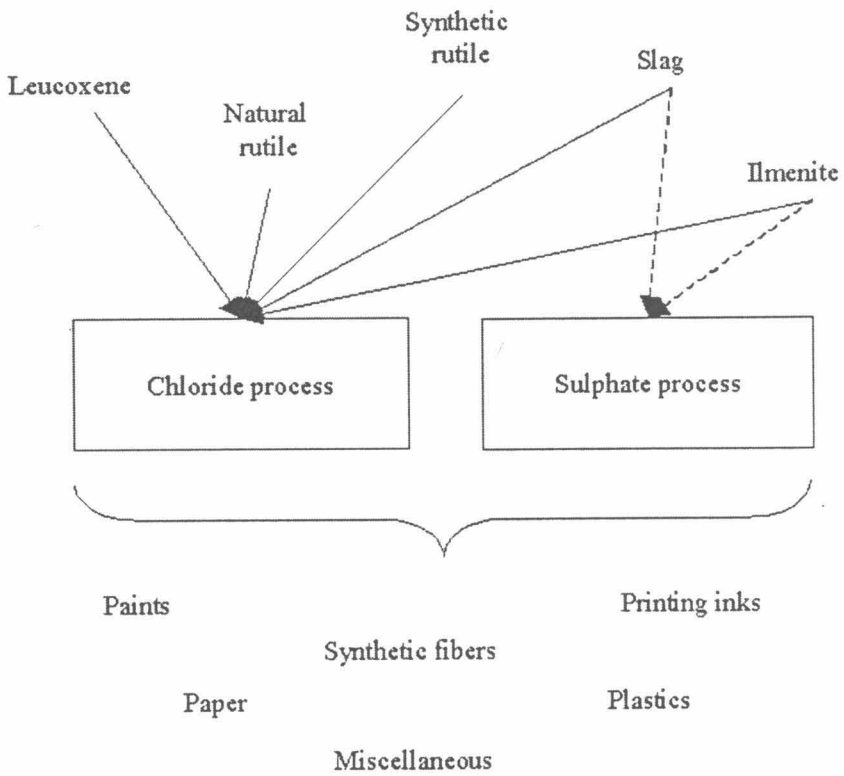

Figure 2.2: Overview of the link between the TiO_2 pigment industry and the titanium containing feed materials industry (after Fisher 1997).

The heavy minerals industry provides the titanium containing feed material for the production of TiO_2 pigment. As the consumption of TiO_2 pigment rises the demand for TiO_2 feed materials for the pigment production plants increases. High TiO_2 slag is one of the raw materials supplied by the heavy minerals industry to TiO_2 pigment production plants (Fisher 1997). High TiO_2 slag is produced in smelting furnaces by reducing ilmenite with a carbonaceous reductant (Pistorius, 1999). Other titanium containing feed materials include natural rutile, synthetic rutile, leucoxene and ilmenite (Fisher 1997).

The TiO_2 feed materials have to meet a number of chemical composition requirements set by the pigment producers and based on the impact the chemical components have on the operation or final pigment quality. The requirements for feed materials for the sulphate TiO_2 pigment production process are described below (Fisher 1997).

- *Heavy metals*: Most of them end up as contaminants in the final TiO_2 pigment product or waste acid. Chromium and vanadium can degrade the optical properties of the pigment and their presence in the waste acid makes it difficult to dispose of or to recycle into useful products. Phosphorus, manganese and niobium should also be avoided.
- *Fe^{3+}*: Will absorb on the TiO_2 pigment particle and discolour it. It is reduced in the sulphate process by adding iron scrap. Its presence in the feed materials therefore increases production costs, and lower is better.
- *Ti^{3+}*: In this process Ti^{3+} forms Ti_2O_3, which reports to the waste stream resulting in losses of Ti^{3+} units.
- *Clay*: Levels should be as low as possible to minimize digest cake dissolving times.

The requirements for feed materials for the chloride TiO_2 pigment production process are described below (Fisher 1997).

- *Silica*: Low silica levels are desirable, as silica is inert in the chlorinator and tends to accumulate, reducing the throughput of the chlorinator.
- *Alkaline earth oxides*: Low alkaline earth oxides levels are definite requirements as the chlorides of these oxides are liquid in the chlorinator, which will agglomerate the fluidizing particles into a viscous mass terminating all chlorination taking place.
- *Arsenic and tin*: Arsenic should be avoided as it ends up in the final TiO_2 pigment rendering it unsuitable for applications in the food and personal care industries. $SnCl_4$ tends to build up in the recycling stream with the same effect on chlorinator throughput as silica.

2.2 Exploitation of heavy minerals resources

Titanium is the ninth most abundant element in the earth's crust. It is found in a number of minerals (table 2.1), of which only ilmenite ($FeTiO_3$), rutile (TiO_2) and leucoxene warrant economic exploitation. Ilmenite and rutile occur mainly in heavy minerals sand deposits but ilmenite is also associated with magnetite, or hematite in some minor instances, in magmatic deposits. For rock deposits to be commercially workable the TiO_2 content of the deposits should range between 17 and 35 per cent and the TiO_2 containing minerals should not be too intimately intergrown with other minerals. For sand deposits as little as 1 per cent TiO_2, when in the form of rutile, can render a deposit commercially workable (Hammerbeck 1992b).

Table 2.1: The main titanium and associated iron oxide minerals (after www.ngu.no/prosjekter/Geode/titanium)

Mineral (end member composition)	% TiO_2 (theoretical)	Physical properties (H= hardness, D= specific gravity)	Occurrence
Ilmenite ($FeTiO_3$)	52.7	H 5.5-6, D 4.7, black, weakly magnetic, trigonal	Common in gabbros and anorthosites; in placers
Magneto-ilmenite	-	-	Ilmenite with intergrowths of magnetite
Hemo-ilmenite	-	-	Ilmenite with intergrowths of hematite
Rutile (TiO_2)	100	H 6-6.5, D 4.2, reddish brown, tetragonal	In eclogites, granites, pegmatites, gneisses and placers
Anatase (TiO_2)	100	H 5.5-6, D 3.9, brown, tetragonal	In altered titanium-bearing rocks and placers
Brookite (TiO_2)	100	H 5.5-6, D 4.1, yellowish brown, orthorombic	In veins and placers
Leucoxene/altered ilmenite	-	H 4-4.5, D 3.5-4.5	Alteration product; mixture of rutile, hematite, titanite, etc.
Perovskite ($CaTiO_3$)	58.9	H 5.5, D 4.1, orthorombic	In some alkaline rocks
Pseudobrookite (Fe_2TiO_5)	-	H 6, D 4.4, brown to black, orthorombic	In various igneous rocks
Titanite ($CaTiSiO_5$)	40.9	H 5-5.5, D 3.5, brownish, monoclinic	Common accessory mineral in a variety of rocks
Hematite (Fe_2O_3)	-	H 5.5-6.5, D 5.3, reddish brown to black, trigonal	Common in a variety of rocks
Ilmenohematite	-	-	Hematite with intergrowths of ilmenite
Magnetite (Fe_3O_4)	-	H 6, D 5.2, black, strongly magnetic, cubic	Common in a variety of rocks
Titanomagnetite	-	-	Some Ti in solid solution in magnetite
Ilmenomagnetite	-	-	Magnetite with intergrowths of ilmenite
Ulvøspinel (Fe_2TiO_4)	35.7	Dark, magnetic, cubic	Exsolves from magnetite-ulvøspinel solid solutions and may be subsequently oxidised to ilmenite

According to Hammerbeck (1992b) in South Africa ilmenite and rutile from magmatic origin occur in the Bushveld igneous complex, in small amounts in kimberlite and carbonite deposits and also as accessory minerals to granite and pegmatite deposits. As part of fossil beach deposits they occur in the Waterberg system and the Karoo system (Bothaville, Wolmaransstad, Delmas and Carolina). As quaternary beach deposits they occur as older red and brown coastal sands, younger dunes and beach sands or in coastal lagoons. The older red and brown coastal sand dunes of Zululand contain from 2 to 25 per cent heavy minerals (7 to 10 per cent on average). The size of the heavy minerals ranges from 75 to 150 micron diameter. The heavy minerals concentrate in the older red and brown coastal sand dunes usually consists of:

- 70 to 80 per cent ilmenite;
- 2 to 5 per cent leucoxene;
- 2 to 5 per cent rutile;
- 8 to 10 per cent zircon;

- 2 to 8 per cent magnetite;
- Trace to 0.3 per cent monazite;
- 1 to 5 per cent garnet, pyroxene etc.

The Cr_2O_3 content of the ilmenite from older red and brown coastal sand dunes of Zululand is comparable to that of the ilmenite found in the Karoo system (0.1 to 0.7 per cent). Other deposits in South Africa and elsewhere contain very low levels of Cr_2O_3. In table 2.2 the typical composition of ilmenite from South Africa and other heavy mineral sands are stated (Hammerbeck 1992b).

Table 2.2: Composition of natural occurring ilmenite from all over the world – after Hammerbeck (1992b)

Per cent	TiO_2	FeO	Fe_2O_3	Cr_2O_3	V_2O_5
South Africa: St Lucia	49.0	32.5	14.3	0.38	-
South Africa: Richards Bay	49.7	36.6	11.1	0.19	0.29
South Africa: Isipingo	46.6	39.5	9.1	0.10	2.76
South Africa: Umgababa	49.9	37.2	10.5	0.16	0.33
South Africa: Sandy Point	50.3	36.5	10.9	0.07	-
South Africa: Morgan Bay	50.0	38.0	13.1	0.05	-
South Africa: West Coast	41.6	34.1	19.7	0.0	0.92
Florida	57.5	12.3	24.6	-	-
Quebec	70.7	12.2	1.5	0.25	0.55
Malaya	53.1	33.6	8.7	0.005	0.02
India	60.6	9.3	24.2	0.12	0.15
Australia	55.4	22.5	11.1	0.03	0.13
Brazil	48.3	32.4	16.6	0.5	0.06

Figure 2.3 depicts, schematically, a generic flow sheet for a heavy minerals sands operation producing high TiO_2 slag, from mining the sand deposit to the smelting stage. The slag is then sold to the TiO_2 pigment producers as described in paragraph 2.1. In the flow sheet in figure 2.3 different mineral properties are exploited, by means of different types of equipment, to produce specific types of mineral concentrates. The sandy, run-of-mine material is produced by water or non-water based mining methods. A heavy mineral concentrate is produced from the run-of-mine material, utilizing size difference and specific gravity properties. Ilmenite is separated from other minerals in the heavy mineral concentrate, based on magnetic susceptibility properties (Balderson 1999). In high chrome heavy mineral deposits i.e. the older red and brown coastal sand dunes of Zululand, the magnetic susceptibility properties of the ilmenite in the crude ilmenite concentrate is enhanced in order to separate the ilmenite from the chromite minerals. The ilmenite is suitable for the production of high TiO_2 slag only when the Cr_2O_3 content of ilmenite concentrate is less than 0.1 per cent (Beukes and Van Niekerk 1999).

2.3 Definition of crude ilmenite and its constituents

For the purpose of this study *crude ilmenite* is defined as an ilmenite-containing concentrate, produced with one or a combination of the methods indicated in figure 2.3, with a Cr_2O_3 content in excess of 0.1 per cent. Crude ilmenite is therefore unacceptable for TiO_2 slag production. Nell and Den Hoed (1997) stated that crude ilmenite, produced from a Southern African East Coast deposit, contains typically 90 per cent ilmenite, 5 per cent Ti-hematite, 3 per cent spinel and 2 per cent silicates by weight, as separate phases. Naturally occurring ilmenite particles can have Fe_2O_3 (hematite) in solid solution in the $FeTiO_3$ matrix (Nell and Den Hoed 1997). The importance of this solid solution will become clearer as the discussion proceeds.

The Cr_2O_3 content of crude ilmenite, produced from a Southern African East Coast deposit, can be as much as 0.3 per cent and is present in spinels of variable composition (Hammerbeck 1992b, Nell and Den Hoed 1997). Dana and Dana (1944) and Deer et al (1966) define the naturally occurring chromite spinel series as variations on the pure spinels magnesiochromite ($MgCr_2O_4$) and chromite ($FeCr_2O_4$). Deer et al (1966) stated that all natural magnesiochromites contain a considerable amount of Fe^{2+} (which replaces Mg^{2+}) and Al^{3+} or Fe^{3+} (replacing Cr^{3+}). In natural chromites a considerable amount of Mg^{2+} replaces Fe^{2+} with generally appreciable replacement of Cr^{3+} by Al^{3+}, but less so by Fe^{3+}. To produce smelter grade ilmenite the Cr_2O_3 containing spinel particles have to be separated from the

ilmenite particles. Various secondary beneficiation methods for crude ilmenite, to separate the chromite from the ilmenite in order to reduce the Cr_2O_3 content of the final ilmenite product, will be described as the discussion proceeds.

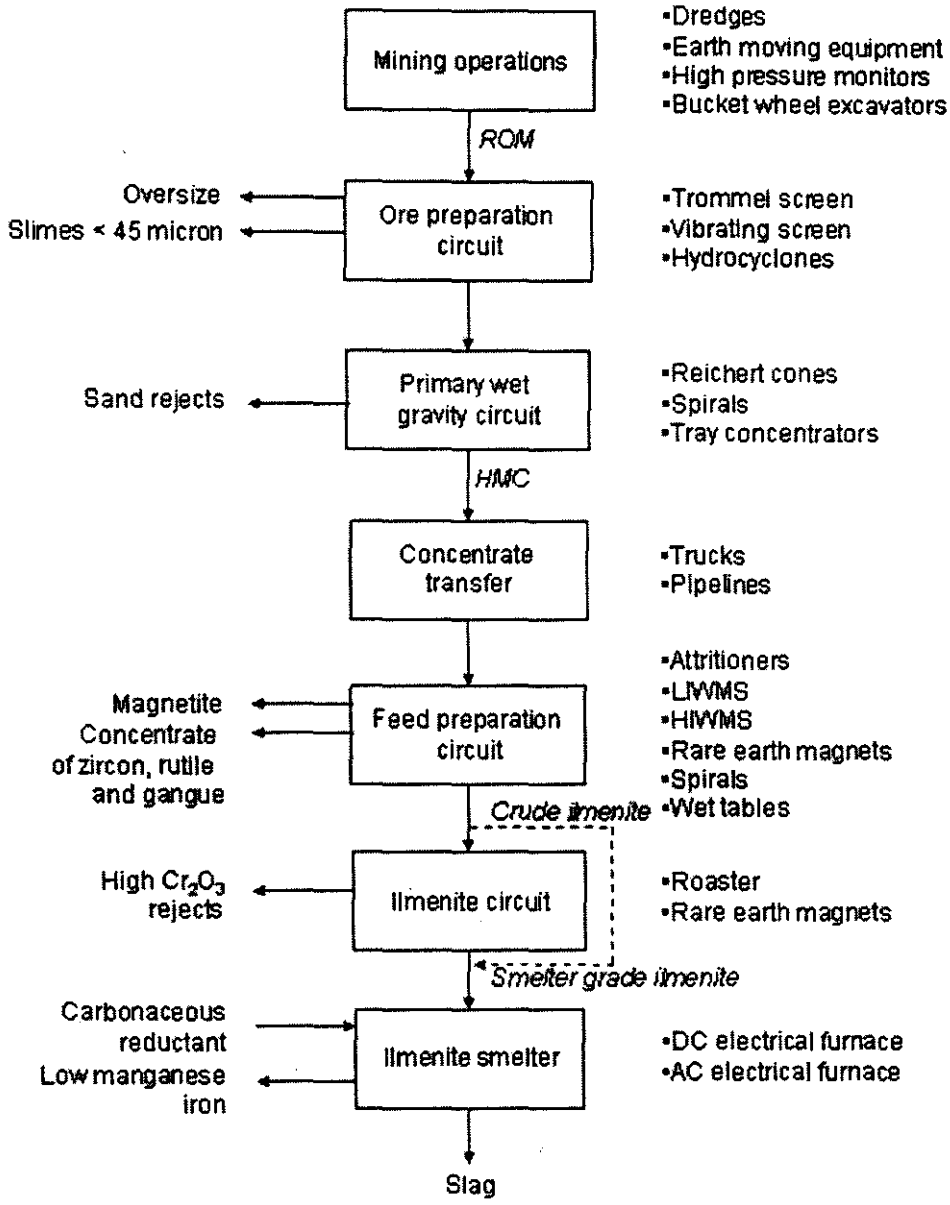

Figure 2.3: Generic flow sheet for a heavy minerals operation producing high TiO_2 slag after Balderson (1999), Beukes and Van Niekerk (1999) and Pistorius (1999).

2.4 Beneficiation of crude ilmenite from Southern African East Coast deposits

According to Kelly and Spottiswood (1995) mineral separation is brought about by suspending particles in a medium and passing this suspension through a suitable piece of equipment named a separator. Liberation of particles is a prerequisite for perfect separation, i.e. all particles that require separation from each other should be discrete particles. In most cases particles are not completely liberated.

Furthermore Kelly and Spottiswood (1995) state that separation depends on three factors:

- The properties of the minerals of which ideally only one is exploited in order to separate particles form each other;

- The characteristics of the separator; and
- Production requirements of grade and recovery – the former determined by the client and the latter by the financial feasibility of the project.

According to Kelly and Spottiswood (1995) in a set of particles there is normally a range in the value of the property being exploited. This range of property values of a given set may be presented as a frequency curve, also known as a separability curve. In a separability curve the fraction of the set of particles with a specific value of property X is expressed as a function of the value of property X. It is important to remember that the separation predicted from separability curves represents the maximum separation that can be achieved, on the material as it exists, by exploiting that particular property. Engineering limitations mean that a separator never achieves the maximum separation indicated by the separability curves, but one may give a better performance than the other (Kelly and Spottiswood 1995).

This study is limited to a single property of the ilmenite and Cr_2O_3-containing spinel minerals, i.e. magnetic susceptibility, which is exploited and manipulated in order to separate the particles from each other. The specific gravity of ilmenite (4.1-5.1 t/m^3) and chromite (4.5-5.0 t/m^3) is very similar. They therefore report to the same stream when using separation methods based on gravity i.e. in the feed preparation circuit as described by Balderson (1999) in figure 2.3.

When a satisfactory displacement does not exist between separability curves, whether no displacement at all or too little displacement, two alternatives exist:

1. Change the distribution of values of X by some pre-treatment;
2. Exploit a different property.

Bergeron and Prest (1974), Nell and Den Hoed (1997) as well as Beukes and Van Niekerk (1999) constructed separability curves for crude ilmenite from Southern African East Coast deposits, represented by TiO_2, and chromite, represented by Cr_2O_3, based on magnetic susceptibility. When the displacement between ilmenite and chromite was not satisfactory the authors of all three papers decided to subject the material to an oxidising roast, i.e. change the distribution of the magnetic susceptibility of the ilmenite by some pre-treatment. All of them produced two sets of curves: one of the mineral concentrate before roasting and one of the mineral concentrate after roasting. Figure 2.4 is reproductions of the two curves from Nell and Den Hoed (1997).

In this study production requirements of grade, as defined by the client and described in paragraph 2.1 and 2.2, play an important role and recovery is referred to but not focussed on in detail.

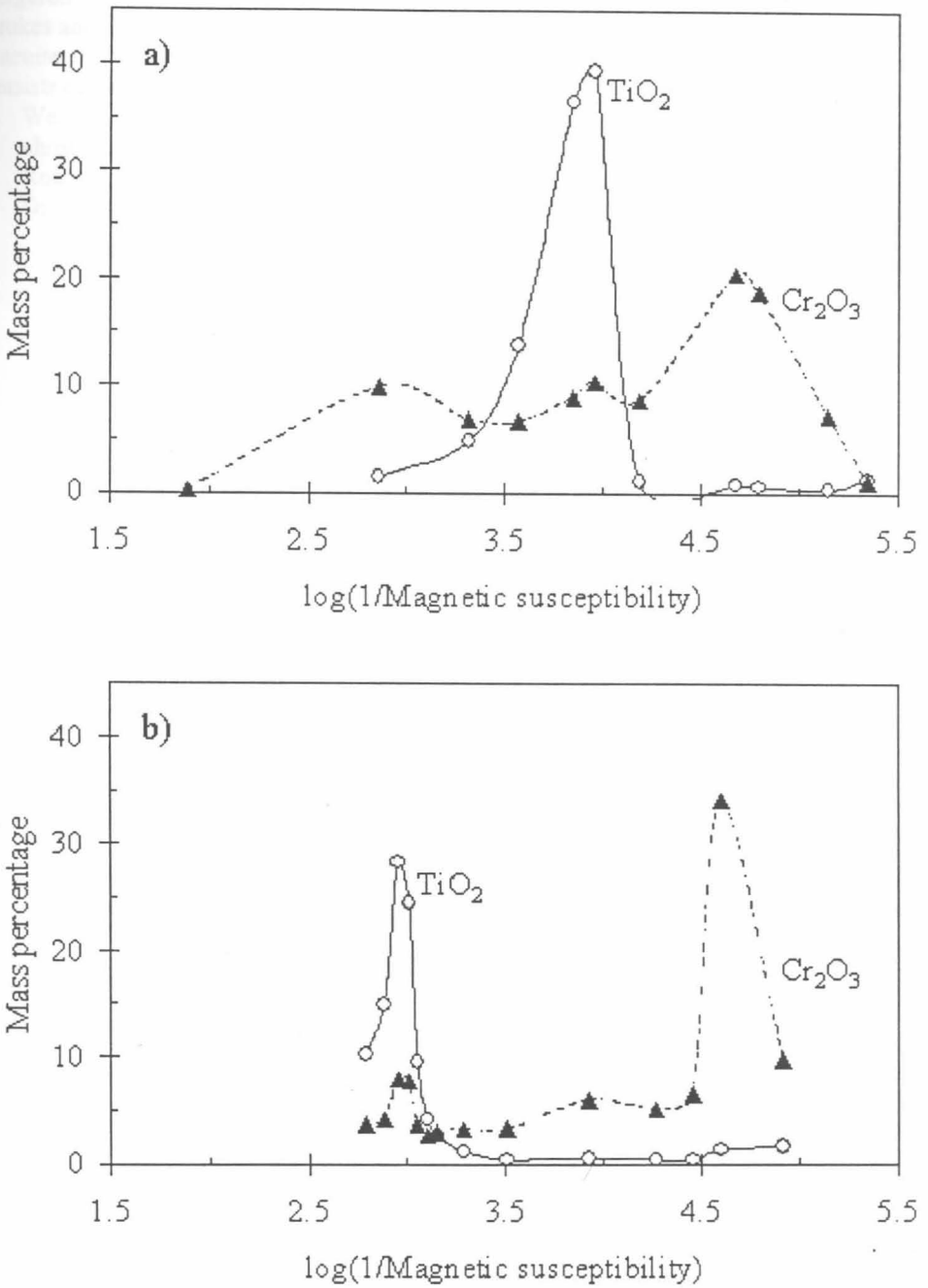

Figure 2.4: TiO_2 and Cr_2O_3 distribution of a) unroasted ilmenite concentrate and b) ilmenite concentrate roasted at 750°C in a mixture of air and CO_2 reported by Nell and Den Hoed (1997). The retention time of the sample in the roasting atmosphere was not reported. Redrawn from the results of Nell and Den Hoed (1997). (Mass magnetic susceptibility in cgs units).

2.5 Description of alternative flow sheets to beneficiate crude ilmenite from Southern African East Coast deposits

In their paper Beukes and Van Niekerk (1999) compared three secondary beneficiation processes for crude ilmenite produced from a Southern African East Coast deposit. Their aim was to produce ilmenite with Cr_2O_3-levels less than 0.1 per cent, from an ilmenite concentrate with Cr_2O_3-levels of the

order of 0.3 per cent. They claimed that the third process described by them, has a lower operational cost than the conventional process patented by Bergeron and Prest (1974).

Bergeron and Prest patented the first process described by Beukes and Van Niekerk (1999) in 1974. Beukes and Van Niekerk (1999) claimed that this process resulted in 80 per cent yield of smelter grade ilmenite with less than 0.1 per cent Cr_2O_3. The process is presented schematically in figure 2.5 and consists of the following three steps:

1. Wet magnetic separation of the crude ilmenite concentrate at 2000-3000 Gauss. In this step chromite with a high magnetic susceptibility reports to the magnetic reject fraction.
2. Roasting the non-magnetic fraction in an oxidizing atmosphere.
3. Dry magnetic separation of the roasted material at 1000-2000 Gauss.

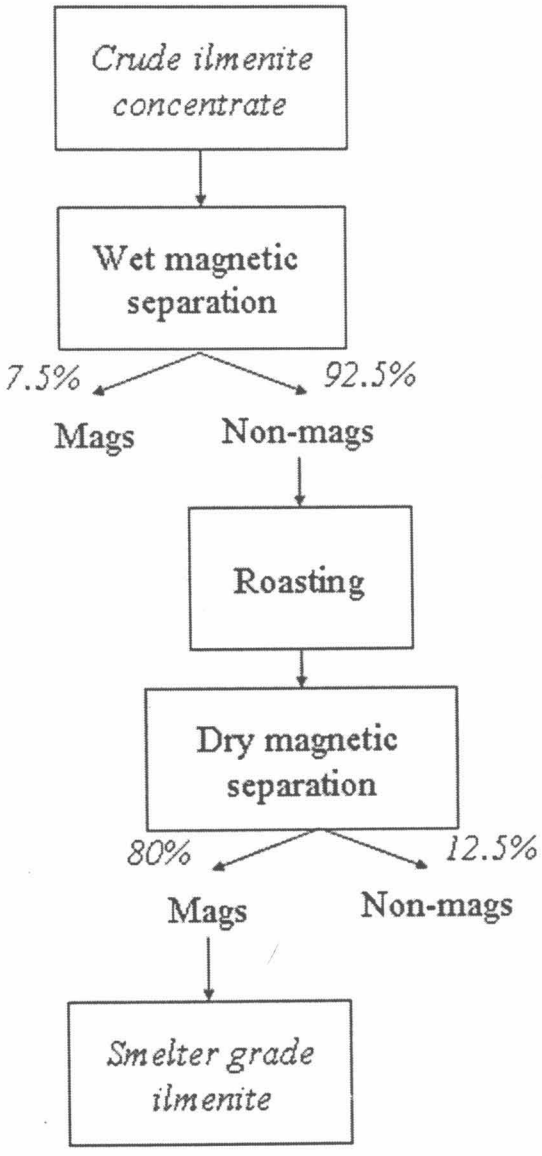

Figure 2.5: Process #1 of the three secondary beneficiation processes for crude ilmenite described by Beukes and Van Niekerk (1999).

The separability curve constructed by Nell and Den Hoed (1997) in figure 2.4b supports the statement made by Beukes and Van Niekerk (1999). In the crude ilmenite concentrate after roasting the TiO_2 is concentrated in a single population with a higher magnetic susceptibility than prior to roasting – refer figure 2.4a - and the Cr_2O_3 retains a bimodal population. A product with less than 0.1 per cent Cr_2O_3 can probably be produced from this concentrate by extracting the TiO_2-containing fraction to the high susceptible side as in the method described by Beukes and Van Niekerk (1999). Nell and Den Hoed (1997) claimed that 90 per cent by weight of the roasted crude ilmenite would report to the magnetic

fraction and the TiO_2 recovery would be 95 per cent. They stated that roasting did not change the magnetic susceptibility of the chromium-rich spinel. The recovery reported by Nell and Den Hoed (1997) is based on laboratory scale studies, which are closer to ideal conditions than the pilot studies conducted by Beukes and Van Niekerk (1999). The studies by Beukes and Van Niekerk are closer to the performance of industrial scale plants.

The second process described by Beukes and Van Niekerk (1999) is depicted in figure 2.6. Beukes and Van Niekerk (1999) claimed that this process resulted in 70 per cent yield of smelter grade ilmenite with less than 0.1 per cent Cr_2O_3. The process consists of the following three steps:

1. Drying of the crude ilmenite concentrate.
2. Dry magnetic separation of the dried crude ilmenite concentrate at 2350 Gauss.
3. Dry magnetic separation of the non-magnetic fraction at 6500 Gauss.

The main differences with the first process are hence that no roasting is performed and the 'cleaning' separation step is performed at a higher field strength.

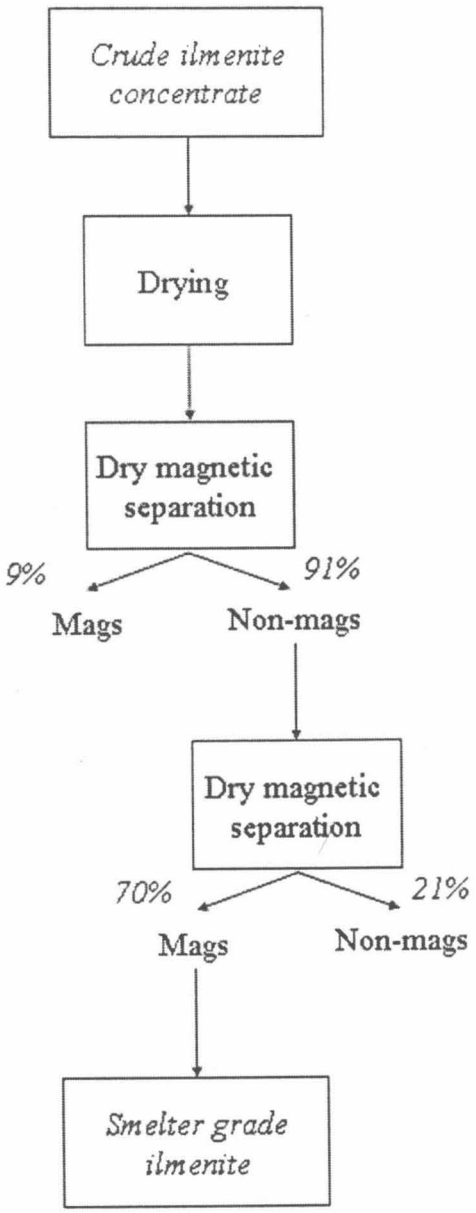

Figure 2.6: Process #2 of the three secondary beneficiation processes for crude ilmenite described by Beukes and Van Niekerk (1999).

The separability curve constructed by Nell and Den Hoed (1997) in figure 2.4a supports the statement made by Beukes and Van Niekerk (1999). In the crude ilmenite concentrate prior to roasting the TiO_2 is concentrated in a single population and the Cr_2O_3 in a bimodal population. A product with less than 0.1 per cent Cr_2O_3 can probably be produced from this concentrate by extracting the TiO_2-containing fraction which lies between the bimodal distributions of chromite, as in the method described by Beukes and Van Niekerk (1999). Nell and Den Hoed (1997) did not discuss this option and therefore no laboratory scale mass or TiO_2 recoveries for this option is available.

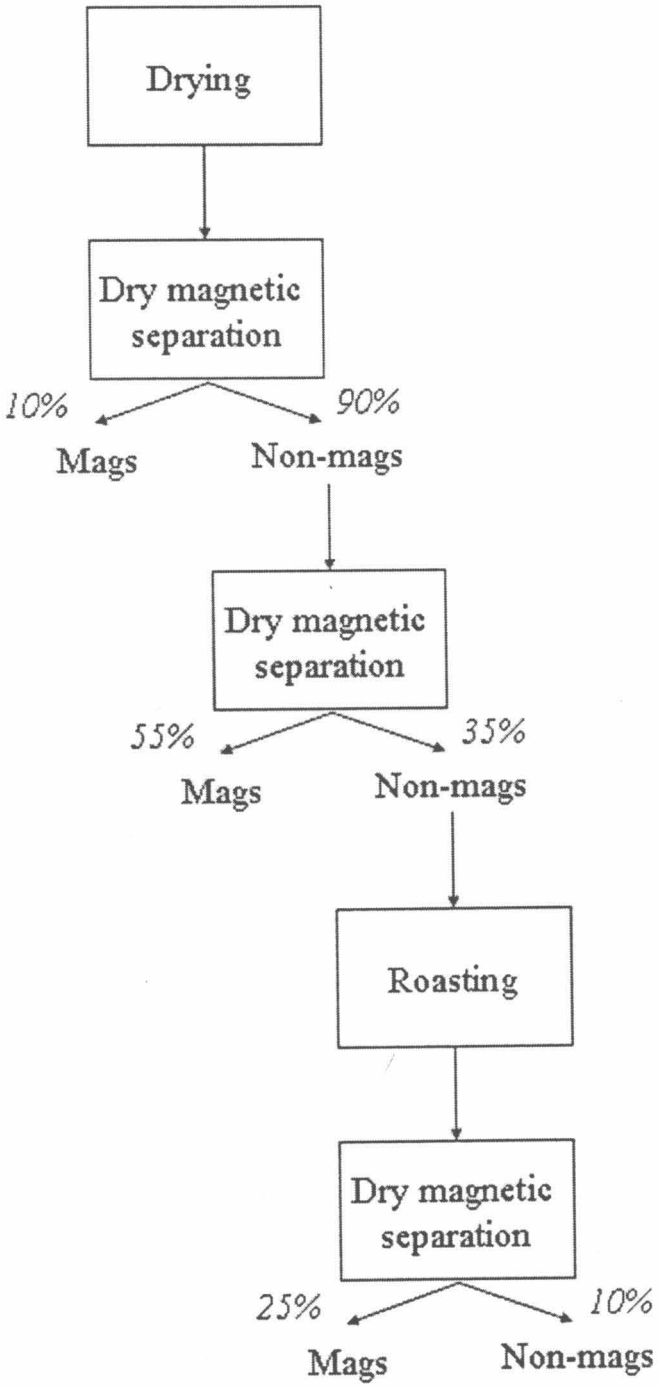

Figure 2.7: Process #3 of the three secondary beneficiation processes for crude ilmenite described by Beukes and Van Niekerk (1999).

The third process described by Beukes and Van Niekerk (1999) is depicted in figure 2.7. They claimed that this step resulted in 80 per cent yield of ilmenite with less than 0.1 per cent Cr_2O_3. This recovery

figure is similar to that obtained in Process #1 but with less material requiring roasting. The process consists of the following five steps:

1. Drying of the crude ilmenite concentrate.
2. Dry magnetic separation of the dried crude ilmenite concentrate at 2350 Gauss.
3. Dry magnetic separation of the non-magnetic fraction at 6500 Gauss.
4. Roasting of the non-magnetic fraction – for the purpose of this study referred to as LSR[1] - in an oxidizing atmosphere.
5. Dry magnetic separation of the roasted material at 1000-2000 Gauss.

The process is hence similar to Process #2, but with an additional roasting and magnetic separation step.

Beukes and Van Niekerk (1999) proposed that because the ilmenite distribution concentrated to the high-susceptibly side after roasting and the chromite distribution remained bi-modal and did not change during oxidizing roasting (as stated by Nell and Den Hoed 1997), the roasting of the LSR would render the ilmenite magnetic and the chromite non-magnetic. If that were the case it would be possible to separate the ilmenite from the chromite. The roasting conditions most probably would be similar to that for crude ilmenite published by Nell and Den Hoed (1997) or Bergeron and Prest (1974). This led to the decision to test the hypothesis in the work presented here:

"It is possible to produce an ilmenite product suitable for ilmenite smelting by subjecting LSR to roasting and subsequent magnetic separation, using the roasting conditions recommended for crude ilmenite by Nell and Den Hoed (1997) or Bergeron and Prest (1974)"

The following are quotes on the behaviour of chromite during oxidising roasting of chromite containing ilmenite concentrates:

"...roasting does not increase the magnetic susceptibility of the other minerals present in the concentrate and specifically that of chromium-bearing spinel..." - Nell and Den Hoed (1997).

and

"...At the same time the chromite phase, the major Cr_2O_3 contaminant in the ore, remains relatively unchanged..." - Bergeron and Prest (1974)

The statements in these quotes led to the decision to test the second hypothesis in the work presented here:

"The magnetic susceptibility of chromite remains constant during magnetizing roasting of an ilmenite concentrate under the oxidizing conditions reported by Nell and Den Hoed (1997)."

2.6 Description of the principles of magnetic beneficiation

The dominant external force on a particle in a magnetic separator is the magnetic force. The separation of one mineral from another depends on the motion of the particle in response to this magnetic force vs. the motion of the particle in response to other competing forces. The competing forces include gravitational, hydrodynamic drag, inertial, friction and centrifugal (in the case of rotating drum separators) forces as well as interparticle forces of electromagnetic and electrostatic origin. The importance of each competing force is a function of the type of magnetic separator and the properties of the particles involved. To ensure separation between minerals with strong magnetic properties and minerals with less strongly magnetic properties, the magnetic force acting on the strong magnetic mineral (F^m_{mag}) must be greater than the sum of the competing forces ($\sum F^m_c$). Likewise for the mineral with less strongly magnetic properties the magnetic force acting on the strong magnetic mineral (F^n_{mag}) must be less than the sum of the competing forces ($\sum F^n_c$) – refer to equation 2.1.

A) $\mathbf{F^M_{MAG} \geq \sum F^M_C}$

B) $\mathbf{\sum F^N_C \geq F^N_{MAG}}$

[1] LSR is the abbreviation of Low Susceptibility rejects

Equation 2.1: Conditions to be met in a magnetic separator to ensure efficient separation of the magnetic minerals from non-magnetic minerals (Svoboda, 1987)

Hayes (1993) divided magnetic separation processes into high (>100 Am^{-1}) and low (<10 Am^{-1}) intensity processes. Hayes (1993) stated that low intensity processes are used to separate materials with high magnetic susceptibilities from materials with low susceptibilities (e.g. Fe_3O_4 from SiO_2). Likewise high intensity processes are used to separate materials with weak magnetic susceptibilities from process streams.

When feeding slurry into a magnetic separator, two streams should exit it: one consisting of magnetic minerals and the other of non-magnetic minerals (Kelly and Spottiswood 1995; Svoboda 1987). In real separation not only are there three streams – magnetic, middlings and non-magnetic – but both magnetic and non-magnetic minerals also report to all three streams. Separation is complete in very limited cases (Svoboda 1987). Figure 2.8 is a schematic presentation of the ideal vs. real magnetic separator.

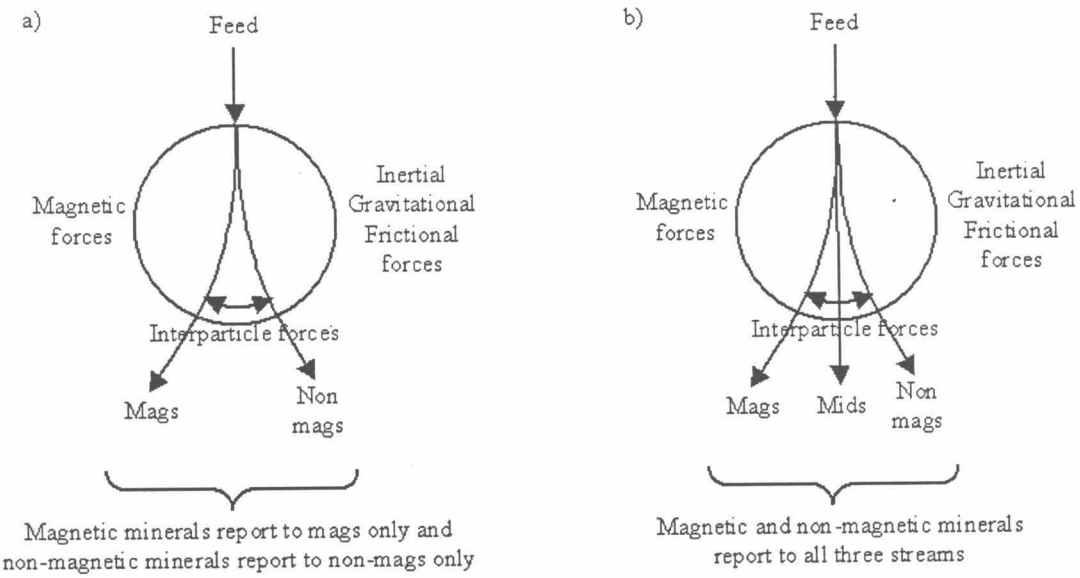

Figure 2.8: Schematic representation of a) an ideal and b) a real magnetic separator after Svoboda (1987).

2.7 Description of the principles in magnetization

2.7.1 Magnetization, magnetic force and magnetic susceptibility

Hayes (1993) stated that the magnitude of the interaction of a material with a magnetic field is often described in terms of magnetic susceptibility, Svoboda (1987) defined both volume magnetic susceptibility (κ) and specific or mass magnetic susceptibility (χ). In equation 2.2,

$$a)\ M=\kappa H$$

$$b)\ J = \mu_o \kappa H$$

Equation 2.2: Definition of volume magnetic susceptibility (Svoboda 1987)

κ is the magnetization per unit field or the volume magnetic susceptibility of an isotropic material in equilibrium in a magnetic field strength H, with a magnetization M along the field direction. The unit of measurement of volume magnetic susceptibility is dimensionless. In equation 2.3,

a) $\kappa = \rho\chi$
therefore b) $\chi = \kappa/\rho$
and eq 3a) into b) $\chi = M/H * 1/\rho$

Equation 2.3: Definition of mass or specific magnetic susceptibility (after Svoboda 1987 and Hayes 1993)

χ is the mass or specific magnetic susceptibility with respect to the unit mass of material with a density ρ. The unit of measurement of specific magnetic susceptibility is m^3kg^{-1}.

Svoboda (1987) summarized the relationships between the different systems of units that magnetic susceptibility was expressed in literature. These relationships were stated in equation 2.4:

a) $\kappa(SI) = 4\pi\kappa(cgs)$
b) $\kappa(cgs) = \rho\chi(cgs)$
c) $\kappa(SI) = 4\pi\rho\chi(cgs)$
d) $\chi(SI) = 4\pi*10^{-3}*\chi(cgs)$

Equation 2.4: Summary of the relationships between the different systems of units that magnetic susceptibility as expressed in literature (Svoboda 1987)

In table 2.3 the conversion factors between volume and specific magnetic susceptibilities are stated in both SI and cgs systems (Svoboda, 1987).

Table 2.3: Definitions and units of measurement used in the definition of magnetic susceptibility – Sears et al (1986); Kelly and Spottiswood (1995) and Svoboda (1987)

Symbol	Definition	SI unit	Cgs unit	Conversion factor F^2
B	Magnetic induction	Tesla [T]	Gauss [G]	10^{-4}
H	Magnetic field strength	$[A.m^{-1}]$	Oersted [Oe]	$10^3/4\pi$
J	Magnetic polarization	Tesla [T]	[emu cm^{-3}]	$4\pi * 10^{-4}$
M	Magnetization	$[A.m^{-1}]$	[emu cm^3]	10^3
μ_0	Magnetic permeability of a vacuum/free space	$[Hm^{-1}]$	1	$4\pi \times 10^{-7}$
	Magnetic flux	Weber [Wb]	Maxwell [Mx]	10^{-8}
κ	Volume magnetic susceptibility	-	-	$1/4\pi$
χ	Specific (mass) magnetic susceptibility	$[m^3\ kg^{-1}]$	[$cm^3\ g^{-1}$ (or emu g^{-1} or emu $g^{-1}cm^{-3}$)]	$1000/4\pi$
μ_m	Magnetic moment	$[Tm^3]$	[emu]	$4\pi10^{-10}$
σ_m	Specific polarization	$[Tm^3kg^{-1}]$	[emu g^{-1}]	10^{-7}
r	Distance between source point and field point	m	M	
v	Velocity vector of q	ms^{-1}	ms^{-1}	
θ	Angle between vector v and line qP	°	°	
k'	Proportionality constant	-	-	$\mu_0 4^{-1}\pi^{-1} = 10^{-7}$

Svoboda (1987) stated that most equations used volume magnetic susceptibility, but that experimentally it would be easier to determine mass or specific magnetic susceptibility. All experimental magnetic susceptibility measurements in this study were based on mass or specific magnetic susceptibility (χ) and results were reported in cgs units as $cm^3\ g^{-1}$.

As the type of magnetic separator to be used in this study is a Frantz isodynamic separator, the only competing force would be gravitational. Svoboda (1987) mathematically described the gravitational force on a spherical particle with radius b of density ρ_p as in equation 2.5.

[2] F is the number by which the quantity in cgs units must be multiplied to obtain the quantity in SI units, i.e. SI = cgs x F

$$F_g = {}^4/_3\pi(\rho_p - \rho_f)b^3g$$

Equation 2.5: Mathematical definition of the magnitude of the competing gravitational force acting on a particle in a magnetic separator Svoboda (1987)

Where ρ_f is the density of the fluid medium and g the acceleration of gravity. When dry separation takes place the value of ρ_f is zero. Svoboda (1987) also gave an equation for the hydrodynamic drag force, which would be a factor in any wet magnetic separation applications. Both the traction magnetic force and the competing gravitational force are functions of particle size. Therefore the larger the particle size the greater the influence of the gravitational force. Separation based on differences in magnetic susceptibility would only be possible for a narrow interval of particle size where separation conditions are optimum (Svoboda 1987).

2.7.2 Paramagnetic, diamagnetic and ferromagnetic materials

All matter responds to the presence of the external magnetic field, although the degree of the response varies considerably. The applied magnetic field interacts with the magnetic field of the atoms of the matter, which exists as a consequence of:

- The precessional motion of the charged nucleus;
- The orbital motion of the electrons around the nucleus and;
- The spin motion of electrons and nuclei (Svoboda 1987).

Svoboda (1987) stated that according to their properties minerals could be divided into three basic groups: ferromagnetic; paramagnetic and diamagnetic. Smith (1990) described two other groups: ferrimagnetic and antiferromagnetic. Hayes (1993) stated that for practical purposes ferro-, ferri- and antiferromagnetic material could be regarded as special cases of paramagnetic materials.

Prior to the development of HGMS (High Gauss Magnetic Separators) the technological classification for magnetic separation differed from the fundamental physical categorization (Svoboda 1987):

- *Strongly magnetic minerals*: minerals, such as magnetite, which could be recovered by a magnetic separator using a relatively weak magnetic induction of up to 1500 Gauss. The responding magnetic susceptibility of these minerals would be greater than $5*10^{-5}$ m^3kg^{-1} ($4*10^{-3}$ cm^3g^{-1});
- *Weakly magnetic minerals*: minerals, such as iron and manganese oxides and carbonates as well as ilmenite, which could be recovered by a magnetic separator using a relatively weak magnetic induction of up to 8000 Gauss. The responding magnetic susceptibility of these minerals ranged from $5*10^{-6}$ down to $1*10^{-7}$ m^3kg^{-1} ($4*10^{-4}$ down to $8*10^{-6}$ cm^3g^{-1}). This broad group of minerals included ferrimagnetic and paramagnetic minerals and paramagnetic minerals with parasitic ferromagnetism;
- *Nonmagnetic minerals*: all minerals that could not be recovered by conventional magnetic separators, but which could be recovered by HGMS's. This group of minerals included diamagnetic minerals, which have a negative magnetic susceptibility. The responding magnetic susceptibility of these minerals was less than $1*10^{-7}$ m^3kg^{-1} ($8*10^{-6}$ cm^3g^{-1}).

Each electron spinning on its own axis behaves as a magnetic dipole (Smith 1990). In most cases electrons in atoms are paired and therefore the positive and negative magnetic moments cancel. In *diamagnetic* materials the presence of an external magnetic field slightly unbalances the orbiting electrons and creates small magnetic dipoles within the atoms which are opposite in direction to the external magnetic field (Smith 1990). They therefore repel the external magnetic field, have relative permeability less than unity and negative magnetic susceptibilities - refer to table 2.4 (Kelly and Spottiswood 1995).

Svoboda (1987) explained diamagnetism differently and stated that the electrical charges partially shield the interior of the body from an applied magnetic field. The electron orbits the nucleus in the presence of the central electrostatic field in the atom. When an external magnetic field is applied, the induced current produces a magnetic field opposite to the applied field – according to Lenz's law stated in equation 2.6. According to Svoboda (1987) diamagnetism is present in all substances. It exists in substances that have neither spin nor orbital magnetic moments and diamagnetic susceptibilities are temperature-independent. Hayes (1993) simplified the definition to minerals which are repelled by a magnetic field and which move to positions of low field intensity.

$$\kappa = -\mu_0 N_a e^2 z \langle r^2 \rangle / (6m_0)$$

Equation 2.6: The volume magnetic susceptibility for a mono-atomic molecule where N_a is the number of atoms per unit volume, e the electronic charge, z the number of electrons in an atom, m_0 the rest mass of the electron and $\langle r^2 \rangle$ the mean square distance of electrons from the nucleus (Svoboda 1987).

Svoboda (1987) stated that the magnetic atoms or ions in *paramagnetic* materials have permanent intrinsic magnetic moments and they occur in low concentrations in the material. Susceptibility arises from the competition between the aligning effect of the applied magnetic field and the randomizing effect of thermal vibrations. The magnetic effect disappears once the material is removed from the external magnetic field (Kelly and Spottiswood 1995). The material becomes magnetized when individual magnetic dipole moments align in the applied magnetic field. The individual magnetic dipole moments could be caused by unpaired electrons (total spin of system is not zero) in atoms or molecules or free atoms or ions with a partly filled inner electronic shell (Smith 1990, Svoboda 1987). The material de-magnetizes when the dipole moments de-align when the applied magnetic field is removed, the magnetic moments are randomly oriented and the overall magnetic moment is zero (Smith 1990, Svoboda 1987). According to the Curie law (equation 2.7) the magnetic susceptibility of a paramagnetic substance is inversely proportional to the temperature. Hayes (1993) simplified the definition to minerals attracted by a magnetic field and which move to positions of high field intensity.

$$\kappa = M/H = \mu_m^2 N_a/(3\mu_0 kT) = C/T$$

Equation 2.7: Curie law with C as the Curie constant (Svoboda 1987)

A *ferromagnetic* material is one in which the magnetic dipoles tend to line up parallel to each other even when no external magnetic field is present i.e. it magnetizes spontaneously. Individual magnetic dipole moments, of unpaired electrons in its atoms or molecules, tend to line up spontaneously (Smith 1990) against the disturbing force of thermal motion (Svoboda 1987). Thermal energy, i.e. heating, causes the magnetic dipoles in ferromagnetic material to deviate from perfect parallel alignment and finally a temperature is reached where the ferromagnetism in the material disappears and the material becomes paramagnetic (figure 2.9). This temperature is the Curie temperature of the material. Below the Curie temperature[3] the material is ferromagnetic and above paramagnetic, independent of whether heating or cooling is taking place (Smith 1990). Ferromagnetic materials have large relative permeability (K_m) values (refer to table 2.4). For ferromagnetic material K_m is not constant. The value of K_m increases as the value of the external magnetic field increases until saturation magnetization is reached. At saturation magnetization nearly all individual magnetic dipole moments have their axes parallel to the external magnetic field. Once saturation magnetization is reached the magnetization of the material, as well as the additional field caused by the material, remains constant irrespective of a further increase in the magnitude of the external magnetic field. Some ferromagnetic materials retain their magnetization once the external magnetic field is removed and can become permanent magnets. A ferromagnetic material is therefore characterized by hysteresis, or irreversibility of magnetization. A magnetized ferromagnetic material can be demagnetized by slow cooling from a temperature above its Curie temperature (Smith 1990).

Kelly and Spottiswood (1995) illustrated the linear relationship between magnetization (M) and the applied magnetic field (H) in paramagnetic and diamagnetic minerals and the non-linear relationship in ferromagnetic minerals in magnetization curves (figure 2.9 and figure 2.10). The linear relationship in paramagnetic and diamagnetic minerals indicates the constant magnetic susceptibility ($M.H^{-1}$) throughout the mineral and confirms that the permeability K_m of the mineral is independent of the applied magnetic field. The non-linear relationship in ferromagnetic materials indicates that the permeability K_m of the mineral, and therefore the magnetic susceptibility ($M.H^{-1}$) thereof, is independent of the applied magnetic field until saturation magnetization is reached.

Table 2.4 indicates examples of the different types of metals and minerals in each group with typical relative permeability values for the group and typical magnetic susceptibility for the material, where available. The minerals mentioned are related to this study.

[3] Also referred to as Curie point

Table 2.4: Examples of the three groups of magnetic materials with typical values of their magnetic susceptibility

Group	Typical values of K_m	Examples (Sears et al 1987)	Magnetic susceptibility @ T = 20°C [$cm^3\ g^{-1}$]	Reference
Diamagnetic	0.99990 to 0.99999	Copper	-1.0×10^{-5}	Sears et al (1987)
		Quartz	-0.45×10^{-6}	Svoboda (1987)
Paramagnetic	1.0001 to 1.0020	Aluminium	2.2×10^{-5}	Sears et al (1987)
		Hematite	$40 - 300 \times 10^{-6}$	Svoboda (1987)
		Ilmenite	$15 - 120 \times 10^{-6}$	Svoboda (1987)
		Chromite	$14 - 69 \times 10^{-6}$	Andres (1976)
Ferromagnetic	1000 to 10000	Iron	Not applicable	Not applicable
		Magnetite	Not applicable	Not applicable

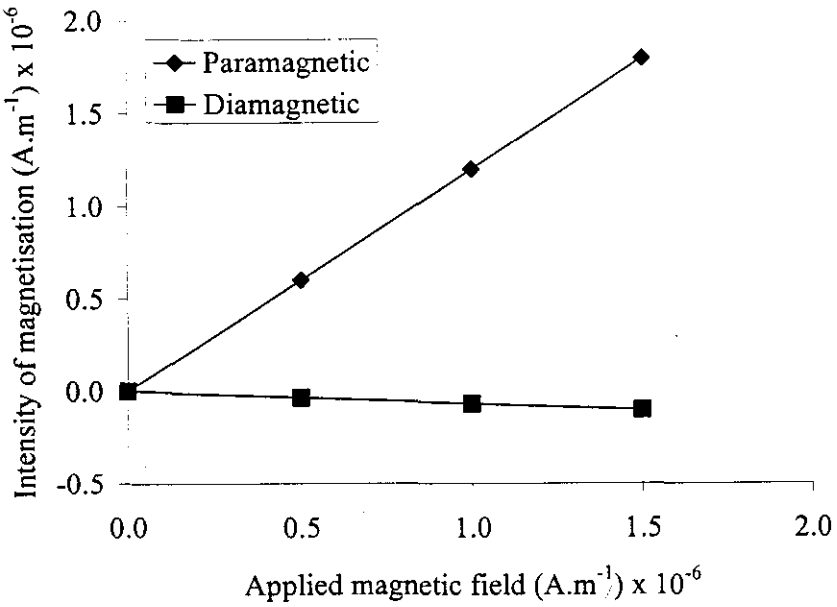

Figure 2.9: Typical magnetisation curves for paramagnetic (hematite) and diamagnetic (quartz) minerals – after Kelly and Spottiswood (1995)

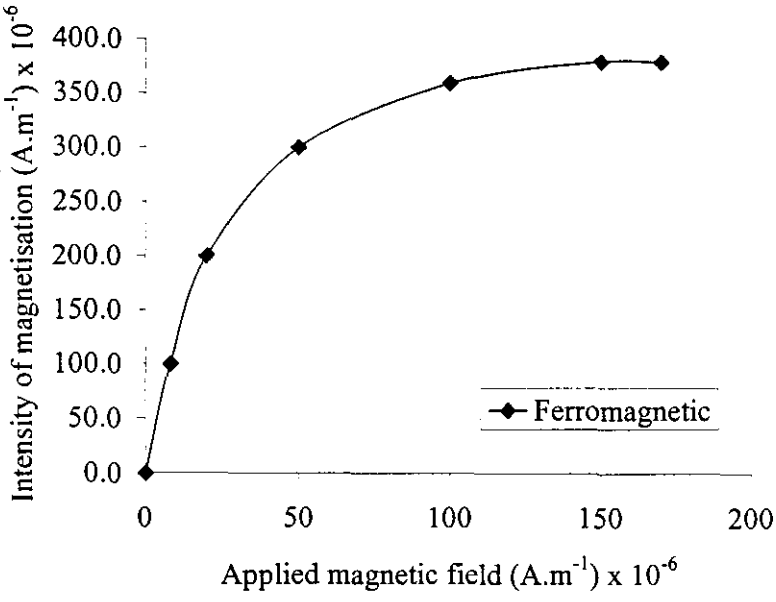

Figure 2.10: Typical magnetisation curves for ferromagnetic minerals (magnetite) – after Kelly and Spottiswood (1995)

2.8 Magnetic susceptibility of chromite

De Waal and Copelowitz (1972) quoted Rait stating that in the system $MgAl_2O_4$-$MgCr_2O_4$-$MgFe_2O_4$ the straight line connecting the point, 30 mole percent $MgFe_2O_4$-70 mole percent $MgAl_2O_4$, with the point, 10 mole per cent $MgFe_2O_4$-90 mole per cent $MgCr_2O_4$, serves as the room temperature magnetic boundary. Therefore chrome spinels richer in $MgFe_2O_4$ than this boundary or rich in Fe_3O_4 are magnetic at room temperature – refer to figure 2.11.

Schwerer and Gundaker (1975) studied the mechanical and thermal effects on the magnetic properties of natural chromites – refer to table 2.5. They observed that mechanical working increased the saturation magnetisation of natural chromites. On crushing Transvaal hard-lumpy grade chromite they observed an increase in the saturation magnetisation on decreasing particle size, but observed that what they called 'high field susceptibility χ' as relatively independent on particle size or therefore crushing treatment. On the other hand Schwerer and Gundaker (1975) observed that the high field susceptibility χ increased upon cooling and that the saturation magnetisation was independent of temperature when taking measurements at room temperature (300 K) and liquid-nitrogen temperature (78 K).

Table 2.5: Composition of the spinel phase in the natural chromite samples studied by Schwerer and Gundaker (1975)

Component	Transvaal Hard Lumpy	Transvaal Low SiO_2	MasInloc
SiO_2	0	0	0
Al_2O_3	16.59	14.38	29.10
CaO	0	0.04	0.04
MgO	8.21	11.26	16.97
Cr_2O_3	47.89	46.78	36.84
FeO	27.11	26.32	16.12
Fe_2O_3	-	-	0
TiO_2	1.42	0.57	0.27
Total	101.22	99.35	99.34

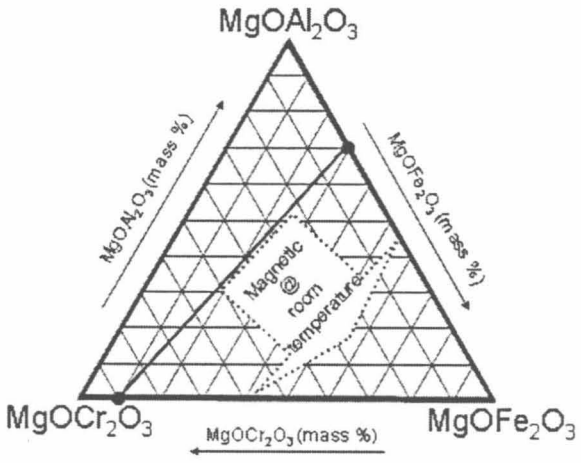

Figure 2.11: The room temperature magnetic boundary of the $MgAl_2O_4$-$MgCr_2O_4$-$MgFe_2O_4$ system (after De Waal and Copelowitz 1972 and Ulmer 1970)

Both the results of the mechanical working and the temperature study indicated the presence of a different phase or structure on the grain surface that differ from the bulk chromite matrix. Schwerer and Gundaker (1975) stated that the measured values of saturation magnetisation was due to a crushing-induced magnetic phase and the high field susceptibility measurements, that of the bulk of the chromite matrix. They attributed crushing-induced magnetisation to changes in surface structures rather than changes in the bulk of the chromite matrix. They stated that the interpretation is compatible with:

- Their observed increased sensitivity to furnace atmosphere at moderate temperatures (270 to 600°C) of crushed material in comparison with annealed material. This was observed when alternating furnace atmosphere between air or He-10 per centH_2 gas mixtures;
- The general absence of chemical unmixing in chromites; and
- The observation of Fe-enriched phases on altered chromite grain surfaces.

Schwerer and Gundaker (1975) compared the changes in magnetic susceptibility of chromite, or lack thereof, with that of iron-titanium oxides. They attributed the changes in the iron-titanium oxides after heat treatments to chemical unmixing at high temperature, phases that are concentrated in magnetic ions with large saturation magnetisation values. This is similar to the mechanism of magnetisation proposed by Guzman, Taylor and Giroux (1992) discussed elsewhere. Schwerer and Gundaker (1975) quoted other authors who stated observations of microscopic veinlets of magnetite in magnetic natural chromite, but could not observe any of these with Mössbauer spectroscopy in the crushed natural chromites. They found that the ordering temperature for the surface structure is about 570°C and stated that it was close to that of magnetite (Fe_3O_4). They stated that the magnetic phase is associated either with Fe-enriched phases or with defect structures on the grain surface. They observed that annealing at temperatures in the range 500-600°C almost fully recovered the crushing induced phase and apparently increase the susceptibility of the chromite grains to gas-solid reactions at moderate temperatures – where the saturation magnetisation of the chromite particles decreased with exposure to an oxidising and increases with exposure to a reducing atmosphere at 430°C.

To summarise the statements made by De Waal and Copelowitz (1972) and the observations made by Schwerer and Gundaker (1975) that are relevant to this study:

- The bulk of the chromite matrix in the natural chromites studied by Schwerer and Gundaker (1975) was paramagnetic;
- Schwerer and Gundaker (1975) observed a mechanically induced surface structure was formed after crushing;
- The surface structure observed by Schwerer and Gundaker (1975) displayed ferromagnetic behaviour. This could have been Fe_3O_4, but this was not proven by the measurement techniques used in the study and the effect was removed during annealing i.e. it might well have been surface defect structures.
- The saturation magnetisation of the ferromagnetic phase, when heat-treated at 430°C (duration not stated), increased in a reducing atmosphere and decreased in an oxidising atmosphere, but no

observations on increase or decrease in bulk magnetic susceptibility when subjecting the chromite to oxidising roasting atmospheres were made (Schwerer and Gundaker 1975).

- Chrome spinel richer in $MgFe_2O_4$ than the boundary created by the straight line connecting the point, 30 mole percent $MgFe_2O_4$-70 mole percent $MgAl_2O_4$, with the point, 10 mole per cent $MgFe_2O_4$-90 mole per cent $MgCr_2O_4$, or rich in Fe_3O_4, are magnetic at room temperature (De Waal and Copelowitz 1972). It is therefore expected that an increase in the Fe_2O_3 or Fe_3O_4 content of a chromite mineral will lead to an increase in the magnetic susceptibility thereof.

2.9 Mechanism of magnetic susceptibility changes in ilmenite

2.9.1 Ferrian ilmenite

According to Dunlop (1990) the most important terrestrial magnetic minerals are oxides of iron and titanium. Figure 2.12 is a ternary phase diagram of these oxides and their solid solution series.

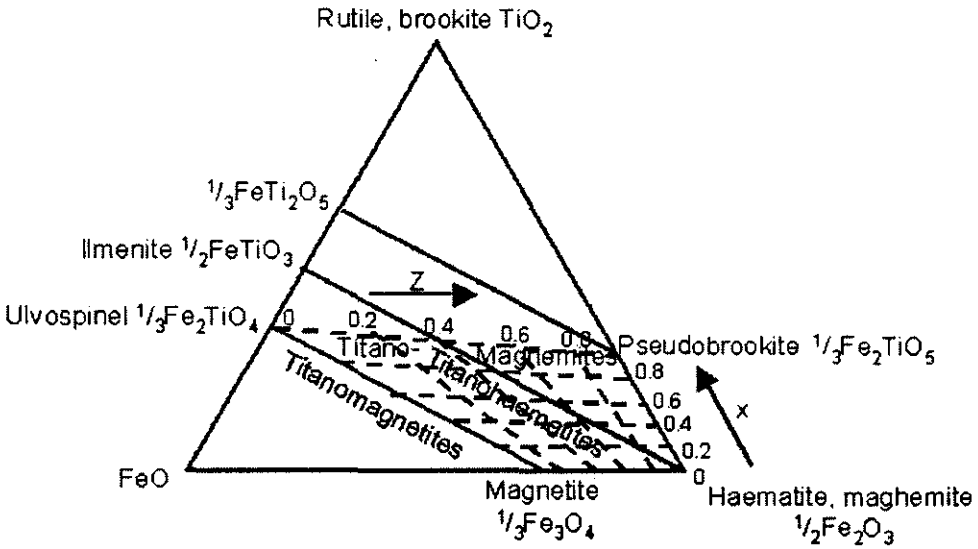

Figure 2.12: Ternary phase diagram of iron-titanium oxides and their solid solution series, x is the Ti content in the titanomagnetites series and z is the oxidation parameter for titanomaghemites (derived from Dunlop 1990).

The ferrian ilmenites ($Ti_yFe_{2-y}O_3$) have compositions between the end-members haematite (αFe_2O_3) and ilmenite ($FeTiO_3$) of which the solid solution is only complete at high temperatures. According to Nord (1989) solid solution between haematite (αFe_2O_3) and ilmenite ($FeTiO_3$) is complete (miscibility is reached) at temperatures above 700°C. Bozorth et al (1957) stated that the solid solution series of $FeTiO_3$-Fe_2O_3 have strong ferromagnetic properties although both end members ($FeTiO_3$ and Fe_2O_3) are paramagnetic or antiferromagnetic (Ishikawa and Akimoto, 1957). According to Dunlop (1990) single-phase ferrian ilmenites of intermediate composition can be preserved by rapid chilling from the solid-solution range. Unlike other ferromagnetic materials the single-phase ferrian ilmenites do not become demagnetised when they are cooled from their Curie temperatures but remain magnetised to some extent. Furthermore the direction of their magnetisation is opposite to that of the field applied during cooling.

2.9.2 Crystal structure of ferrian ilmenites

Dunlop (1990) states that ferrian ilmenites have a corundum structure (i.e. similar to Al_2O_3) with oxygen anions in the hexagonal close-packed lattice and Fe and Ti cations occupying two-thirds of the interstices – figure 2.13. Corundum (Al_2O_3), as ilmenite ($FeTiO_3$), is one of the minerals in the rhombohedral oxide mineral group. The structure of the rhombohedral oxide group consist of hexagonal close packed oxygen with two thirds of the octahedral interstices occupied to give the general formula: A_2O_3.

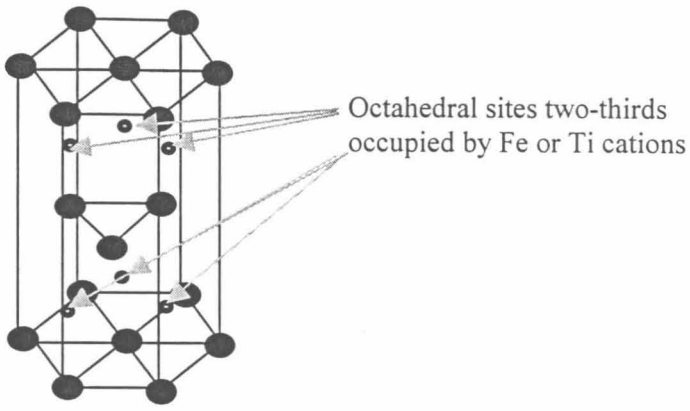

Figure 2.13: Ferrian ilmenites have a corundum structure (similar to Al_2O_3) with O anions in the hexagonal close-packed lattice and Fe and Ti cations occupying only two-thirds of the octahedral interstices to maintain electrical neutrality (after Smith 1990 and Dunlop 1990).

An isolated hexagonal closed packed unit cell has the equivalent of 6 atoms per unit cell (figure 2.14). Three atoms form a triangle in the middle layer; six $^1/_6$-atom sections and one ½-atom section are on both the bottom and top layer. In ferrian ilmenites these atoms are oxygen anions.

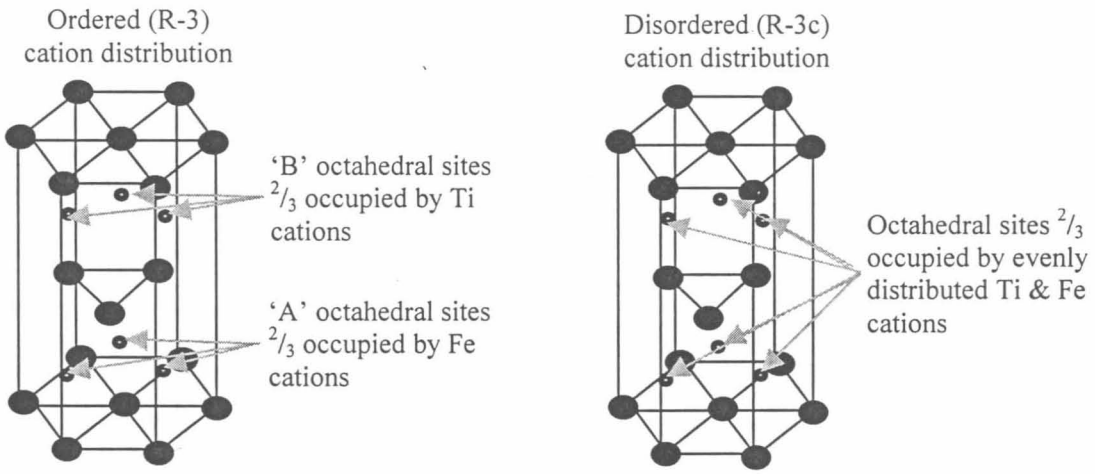

Figure 2.14: The cation distribution of ferrian ilmenites is ordered (R-3) when the Fe and Ti cations are confined to alternate cation (basal) planes and disordered (R-3c) if they are evenly distributed (after Ishikawa and Akimoto 1957b; Dunlop 1990; Smith 1990).

There are voids between the atoms or ions, which are packed into a crystal structure. These voids are interstitial sites where other atoms or ions can be fitted. In the hexagonal closed packed (HCP) structure there are two interstitial sites:

- The octahedral interstitial site, which is formed at the center where six atoms contact each other – indicated in figure 2.15 (Smith 1990);
- The tetrahedral interstitial site, which is formed at the center where four atoms contact each other – not indicated in figure 2.15.

In the HCP crystal structure there are as many octrahedral interstitial sites as there are oxygen atoms and twice as many tetrahedral sites as oxygen atoms (Smith 1990). In ferrian ilmenites the interstitial atoms are iron or titanium cations, which are confined to two-thirds of the octrahedral interstitial sites to maintain charge neutrality (Dunlop 1990). For charge neutrality in A_2O_3 two A^{3+} cations balance three O^{2-} anions and therefore $^2/_3A^{3+}$ balance one O^{2-}.

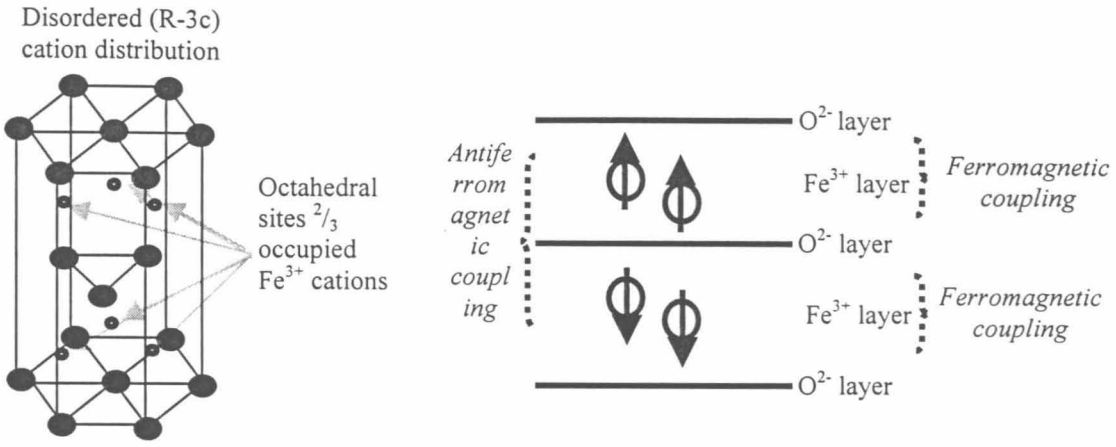

Figure 2.15: The disordered (R-3c) crystal structure of hematite (Fe_2O_3) indicating the distribution of the Fe^{3+} cations. The magnetic coupling due to the crystal structure indicate ferromagnetic coupling within layers and antiferromagnetic coupling between layers (after Ishikawa and Akimoto, 1957b; Bozorth et al 1957 and Banerjee 1991).

2.9.3 Magnetic properties caused by the crystal structure of ferrian ilmenites

a) Order/Disorder

From Dunlop (1990) the cation distribution is ordered (R-3) when the Fe and Ti cations are confined to alternate cation (basal) planes without a center of symmetry. It is disordered (R-3c) if cations are evenly distributed with a center of symmetry – refer to figure 2.16.

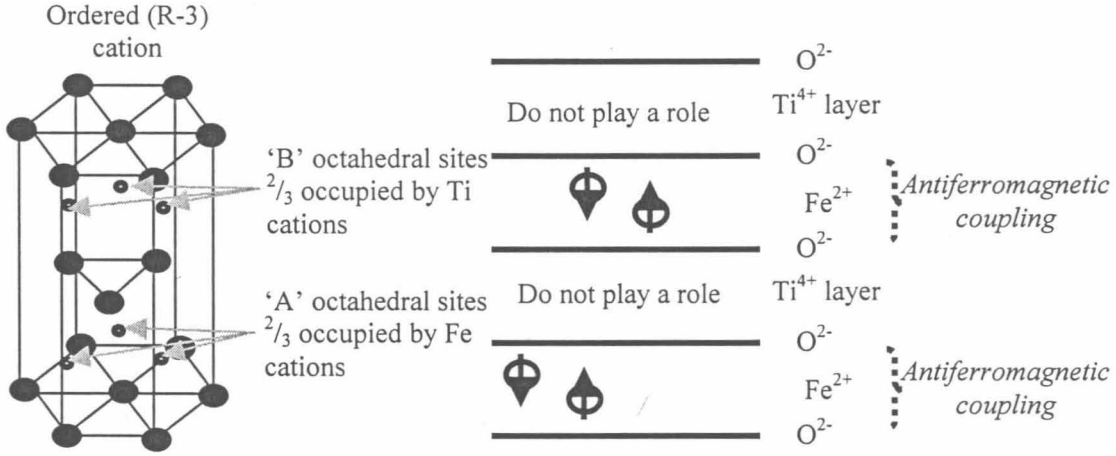

Figure 2.16: The ordered (R-3) crystal structure of ilmenite ($FeTiO_3$) indicating the distribution of the Ti^{4+} and the Fe^{3+} cations. The magnetic coupling due to the crystal structure indicate antiferromagnetic coupling within layers (after Ishikawa and Akimoto, 1957b; Bozorth et al 1957 and Banerjee 1991).

b) Hematite (Fe_2O_3)

Hematite (Fe_2O_3) crystallizes in the corundum (disordered R-3c) crystal structure (Banerjee, 1991) with only Fe^{3+} cations filling $^2/_3$ of the interstitial sites (Bozorth et al, 1957). Bozorth (1957) stated that each Fe^{3+} layer is ferromagnetic in itself and alternating layers antiferromagnetic to each other resulting in zero magnetization. Banerjee (1991) stated that hematite is in principle antiferromagnetic but because

the Fe^{3+} spin moments are slightly canted towards each other, it results in a weak ferromagnetic[4] moment.

c) Ilmenite ($FeTiO_3$)

Ilmenite ($FeTiO_3$) crystallizes in the ordered R-3 hexagonal structure (Banerjee, 1991). Fe^{3+} cations are replaced by Ti^{4+} cations, accommodated in the 'B' planes, and Fe^{2+} cations, accommodated in the 'A' planes as indicated in figure 2.16. This is to conserve charge balance: $2Fe^{3+} = Fe^{2+} + Ti^{4+}$(Banerjee, 1991). Ishikawa & Akimoto (1957) stated that titanium cations are always tetravalent in solid solution and that the Ti^{4+} ions play no part in the magnetic coupling. Both Bozorth (1957) and Ishikawa and Akimoto (1957b) stated that the Fe^{2+} cations are antiferromagnetically coupled *within* each layer. Therefore total magnetization in pure ilmenite is zero (Ishikawa and Akimoto; 1957b). But how then can the magnetic property of ilmenite be used, and improved, to separate it from minerals, which is less magnetic? Banerjee (1991) answered this question by stating that it can either be that one is dealing with titanohaematite solid solutions ($FeTiO_3$ to $Fe_{1.5}Ti_{0.5}O_3$ which is x=0.5 for $xTiFeO_3(1-x)Fe_2O_3$) or that fine-scale ferromagnetic magnetite is exsolved in the ilmenite.

d) Ferrian ilmenites ($xTiFeO_3.(1-x)Fe_2O_3$)

Dunlop (1990) stated that in ferrian ilmenites disordered structures (R-3c) occur for x<0.5 in $xTiFeO_3(1-x)Fe_2O_3$, although not explicitly stated it is assumed that this is at room temperature. Ishikawa and Akimoto (1957b) stated that when quenching ferrian ilmenites after 12 hours of heat treatment from 1200°C to room temperature, disordered structures (R-3c) occur at room temperatures for x<0.5 in $xTiFeO_3(1-x)Fe_2O_3$. Ordered structures (R-3) occur for x>0.5 (Dunlop, 1990; Ishikawa and Akimoto, 1957b). The disordered structures (R-3c) are antiferromagnetic (Dunlop 1990) or feebly ferromagnetic (Ishikawa and Akimoto 1957a). Ishikawa and Akimoto (1957a) observed magnetic induction of 1 to 2 gauss/gram in disordered structures (R-3c). The ordered structures (R-3) are ferrimagnetic (Dunlop 1990) or very strong ferromagnetic (Ishikawa and Akimoto 1957a). Ishikawa and Akimoto (1957a) observed magnetic induction of 30 to 70 gauss/gram in ordered structures (R-3).

Banerjee (1991) stated that the part of the titanohaematite solid solution that is magnetic at room temperature is the $Fe_{1.5}Ti_{0.5}O_3$ to $Fe_{1.27}Ti_{0.73}O_3$ solid solution. Banerjee (1991) stated that this solid solution range is ferrimagnetic and crystallographically ordered, where one cation layer contains iron cations only and the other iron and titanium cations. This layer configuration leads to a net magnetic moment in one direction. Other authors (Ishikawa and Akimoto, 1957b and Bozorth et al, 1957) report other cation configurations with Ti^{4+} cations on both 'A' and 'B' layers, but for the purpose of this study the model proposed by Banerjee (1991) is accepted.

Banerjee (1991) stated that the 3d series (Fe, Mn, Ni, Co etc) are the main magnetic carriers in Fe-Ti oxides but that iron (Fe) is by far the most important source of magnetism. The spin moments for Fe^{3+} and Fe^{2+} are 5 and 4 respectively (Banerjee 1991). This implies that if Fe cations in an 'A' layer are coupled antiferromagnetically the net magnetic moment will not be zero but as in table 2.6. This is actually the definition of ferrimagnetism. The same is true for antiferromagnetic coupling between layers.

Each electron spinning on its own axis behaves as a magnetic dipole and has a dipole moment called the Bohr magneton μ_B (Smith 1990). Bozorth et al (1957) published data where they observed three regions (refer to figure 2.17) based on the Bohr magneton μ_B as a function of the mole fraction Fe_2O_3 (1-X) in the solid solution. Their data were collected for synthetic material, which was either slow cooled or quenched from 1200°C:

- X > 0.85: Little magnetization observed
- 0.5 < X < 0.85: Strong magnetization observed
- X < 0.5: Little magnetization observed

[4] Also referred to as parasitic ferromagnetism

Table 2.6: Net magnetic moment for antiferromagnetic and ferromagnetic coupling between Fe^{3+} and Fe^{2+} cations

Ion	Fe^{3+}	Fe^{2+}
Spin moment (Bohr magneton per molecule)	5	4
Net magnetic moment – antiferromagnetic coupling		5 - 4 = 1
Net magnetic moment – ferromagnetic coupling		5 + 4 = 9

Bozorth et al (1957) stated that although titanomagnetites have a ferrimagnetic order, a threshold amount of Fe_2O_3 must be added to $FeTiO_3$ before the weak antiferromagnetic coupling in the Fe layers of the $FeTiO_3$ is broken down by the stronger antiferromagnetic coupling between layers, as in Fe_2O_3. Bozorth et al (1957) found this threshold value to be 15 mole percent Fe_2O_3 and conducted their measurements from room temperature to 1.3K. Slow cooled samples followed the model proposed by Ishikawa and Akimoto (1957b) more closely than quenched samples, at Fe_2O_3 contents exceeding the threshold value of 15 per cent. The reason for the deviation in quenched samples was given as the preservation of the disordered cation structure (R-3c), which is present at higher temperatures. Nell and Den Hoed (1997) reported results, similar to the curve for slow cooled material reported by Bozorth (1957), for a natural ilmenite concentrate. Nell and Den Hoed (1997) did not describe the cooling method used.

Ishikawa and Akimoto (1957a) observed a similar deviation in the intensity of magnetisation when slow cooling and quenching $0.5TiFeO_3{\cdot}0.5Fe_2O_3$ samples heat treated in a vacuum at different temperatures for 5 hours – figure 2.18. They attributed it to a order-disorder transformation phenomenon, assumed to be R-3c to R-3. Ishikawa and Akimoto (1957a) stated that they suspected this transition temperature to be 600°C (for $0.5TiFeO_3{\cdot}0.5Fe_2O_3$). Nord et al (1989) determined the temperature and composition where the transition between the disordered (R-3c) and ordered (R-3) crystal structure take place as between 1000 and 1050°C for x = 0.7 in the $xTiFeO_3(1\text{-}x)Fe_2O_3$ solid solution.

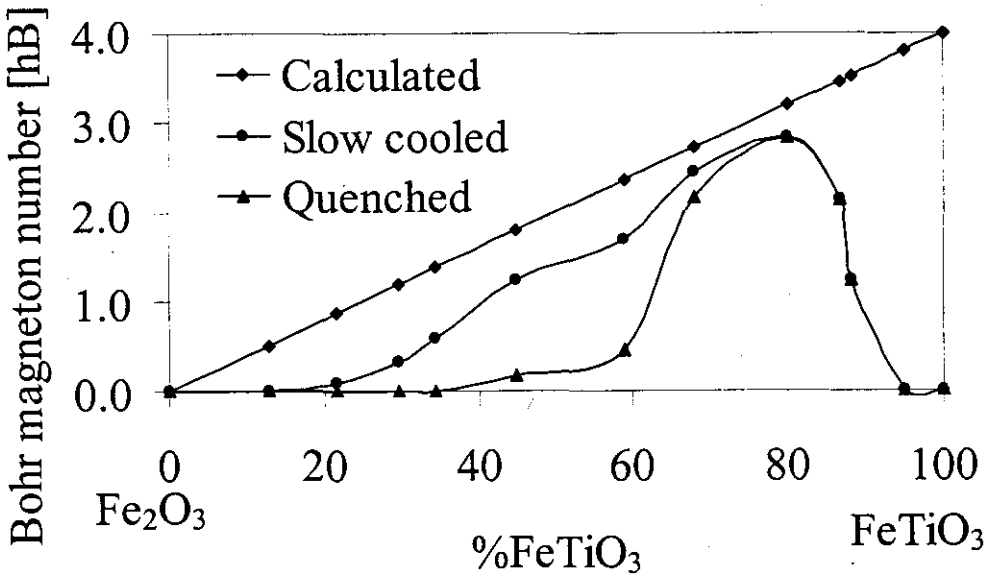

Figure 2.17: Actual Bohr magneton numbers per mole percent Fe_2O_3 in $FeTiO_3$-Fe_2O_3 solid solutions vs. calculated – measured from 1.3°K to room temperature (from Bozorth et al 1957). Compositions plotted as mole percentages.

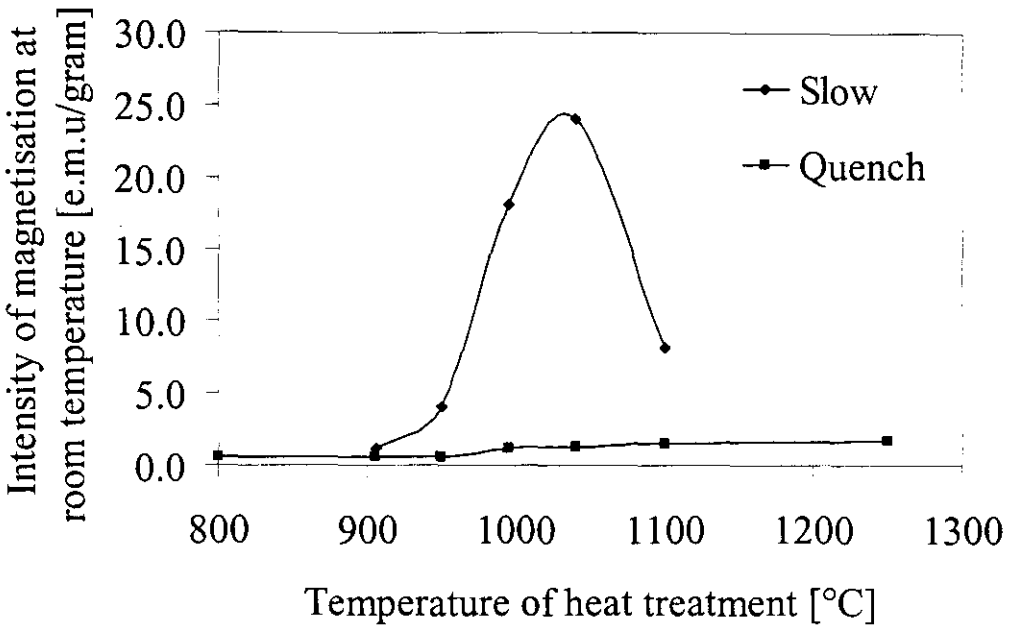

Figure 2.18: Impact of slow cooling or quenching of $0.5TiFeO_3{\cdot}0.5Fe_2O_3$ samples at various temperatures in a vacuum (Ishikawa and Akimoto 1957a).

Nell and Den Hoed (1997) quote Putnis (1992); Nord (1989) and Burton (1984) for a phase diagram for the $xTiFeO_3{\cdot}(1\text{-}x)Fe_2O_3$ solid solution that indicates both the cation crystallographic order/disorder (R-3c/R-3) and the magnetic order/disorder (Curie point) with compositional fields where self-reversing takes place – refer to figure 2.19.

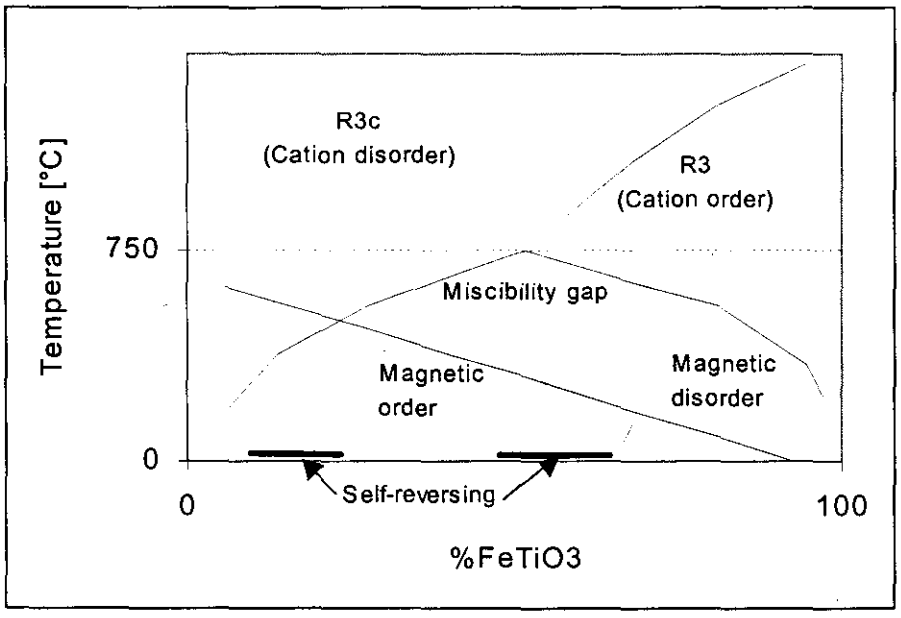

Figure 2.19: Schematic ilmenite-hematite binary phase diagram indicating the R-3c to R-3 cation order-disorder transition, the magnetic order-disorder i.e. the Curie points and the fact that solid solutions in this range are self reversing (Nord et al. 1989).

From this discussion it is concluded that to enhance the magnetic properties of ilmenite ($FeTiO_3$):

- A solid solution of ilmenite and hematite with a minimum of 15 per cent Fe_2O_3 is required, i.e. $x < 0.85$ for $xFeTiO_3(1\text{-}x)Fe_2O_3$ (Bozorth et al, 1957);
- Depending on the cooling rate the maximum amount of Fe_2O_3 in solid solution should be between 40 and 60 per cent, i.e. $x > 0.4$ to 0.6 for $xFeTiO_3(1\text{-}x)Fe_2O_3$, based on results reported by Bozorth et al (1957) and Nell & Den Hoed (1997);

- The crystal structure of the solid solution should be ordered (R-3) – in this instance limiting the maximum amount of Fe_2O_3 in solid solution to either 30 per cent (Nord, 1989) or 50 per cent (Nell & Den Hoed, 1997), i.e. $x = 0.7$ or 0.5 for $x < 0.85$ for $xFeTiO_3(1-x)Fe_2O_3$;
- The solid solution should be below its Curie point to ensure magnetic order. This will be an issue if the Curie point of the solid solution is below operating (room) temperatures.

2.10 Definition of roasting

2.10.1 Roasting in a reducing atmosphere

Walpole (1991) concluded from literature that in ilmenite the maximum magnetic enhancement is achieved when the mole ratio Fe^{3+}:Fe^{2+} is within the range 1:1 - 1.57:1. This is for ferrian ilmenites with $0.56 < x < 0.67$ for $xFeTiO_3(1-x)Fe_2O_3$. For ilmenite with a low Fe^{3+}:Fe^{2+} ratio oxidising conditions would be required to increase the percentage Fe^{3+} in the solid solution and for ilmenite with a high Fe^{3+}:Fe^{2+} ratio, reducing conditions to decrease the percentage Fe^{3+} in solid solution. He claimed that his process of roasting, at 650-900°C for 30-90 minutes using excess carbon, stabilizes the roasting reaction in the zone where Fe^{3+}:Fe^{2+} is within the range 1:1 - 1.57:1. This will be true if:

- The carbon defines the pO_2 in the atmosphere;
- The defined atmosphere is the equilibrium atmosphere for reaction 2.1 with 33-44 mole% Fe_2O_3; in solid solution and
- The following reactions are possible and at equilibrium:

a) $C + \frac{1}{2}O_2 = CO$ (controlling the pO_2 in the atmosphere)
b) $FeTiO_3 + O_2 = Fe_2O_3 + TiO_2$ (Oxidising reaction)
c) $Fe_2O_3 + TiO_2 + CO = FeTiO_3 + CO_2$ (Reducing reaction)

Reaction 2.1: The reactions taking place during ilmenite roasting from Walpole (1991)

(Refer to Appendix 1 at the end of this chapter for details on the calculations stated above).

Nell and Den Hoed (1997) also conducted their study on an ilmenite concentrate from Kwazulu-Natal and reported success when roasting at equilibrium conditions i.e. applying the equilibrium pO_2 at a specific temperature for as long as it requires to reach equilibrium. At 800°C the calculated pO_2 was 10^{-12} bar. The rate of oxidation is very low, though. More than 3 hours were needed at 800°C in 100 per cent CO_2 (measured pO_2 was 10^{-5} bar) to increase the magnetic susceptibility 5-fold. The sample composition was $(FeTiO_3)_{0.6}(Fe_2O_3)_{0.4}$.

Guzman, Taylor and Giroux (1992) patented a reductive roasting process in which magnetic susceptibility is enhanced by roasting at 400-700°C for 8-60 minutes in CO_2 or CO and H_2 gas mixtures. They claimed that the process is especially suitable for ilmenite that have a high Fe_2O_3:FeO ratio. They claimed that a possible explanation for the increase in magnetic susceptibility is the formation of highly magnetic magnetite, i.e. $FeO.Fe_2O_3$, in or on the ilmenite grains.

2.10.2 Roasting in a neutral atmosphere

Grey and Li (2001) reported that some ilmenite concentrates showed a large increase in magnetic susceptibility when roasted in a neutral atmosphere at temperatures higher than 600°C. This was true for altered ilmenite sand concentrates where Fe^{2+}-containing pseudorutile ($Fe_2Ti_3O_9$) was distributed uniformly as a major alteration phase in the ilmenite particle. Grey and Li (2001) postulated that the ferrous pseudorutile contained nanometer scale regions of disordered ilmenite-type structures, which could be transformed at low energy inputs to strongly magnetic ferrian ilmenite (ilmenite containing Fe_2O_3 in solid solution).

2.10.3 Roasting in an oxidative atmosphere

The roasting conditions of the process patented by Bergeron and Prest (1974) was for ilmenite concentrate from Kwazulu-Natal. Their feed material contained 47.5 per cent TiO_2, 36.5 per cent Fe and 0.4 per cent Cr_2O_3. They claimed to decrease the Cr_2O_3 content from 0.4 to 0.1 per cent at a mass recovery of 80 per cent. Their roasting process took place at 690-810°C for 10-45 minutes in the presence of 1-6 percent of excess oxygen over the stoichiometric amount of fuel required. The

preferable roasting conditions were at 750°C for 15 minutes in the presence of 3 per cent excess oxygen, (as mentioned in chapter 1, paragraph 1.2).

Nell and Den Hoed (1997) also conducted their study on an ilmenite concentrate from Kwazulu-Natal and reported excellent results when applying roasting conditions with excess oxygen and terminating roasting before the ilmenite reaches the equilibrium phase composition. In less than 2 hours even at temperatures as low as 700°C the magnetic susceptibility of the ilmenite increased 5- to 6-fold. They also observed a drop in magnetic susceptibility at extended reaction times (i.e. longer than 30 minutes at 800°C). They stated that the rate of oxidation seemed to be more influenced by temperature than by the gas composition in gas mixtures containing more than 1 per cent excess oxygen. As the present study is about oxidative ilmenite roasting I wanted to investigate it further.

2.11 Phase chemical changes during oxidative roasting

2.11.1 Phase diagrams

During the oxidation of ilmenite oxygen atoms are added to the material – refer to reaction 2.1 (Van Dyk 1999). The ratio of titanium and iron remains constant. For theoretical ilmenite this is $N_{Ti}/(N_{Ti} + N_{Fe}) = 0.5$. This is represented schematically in figure 2.20. It is assumed that the ideal roasting conditions for ilmenite concentrate from Kwazulu-Natal is 750°C for 15 minutes in the presence of 3 per cent excess oxygen (Bergeron and Prest, 1974) or within a range of 700°C to 800°C with more than 1 per cent oxygen for 30 minutes or less (Nell and Den Hoed 1997). From the Fe-Fe_2O_3-TiO_2 phase diagrams at 700 & 800°C some conclusions on oxidative ilmenite roasting can be made. These diagrams were constructed from laboratory equilibrium test work. It is important to note that the conditions applied during laboratory scale and full-scale ilmenite roasting are such that equilibrium conditions are not reached. Thermodynamic information on a phase diagram is for equilibrium conditions. Therefore, only an indication of what could happen during ilmenite roasting is obtained from them. From these figures it is concluded that Fe2O3 solid solution in ilmenite is only feasible up to 15-16% Fe_2O_3. This narrows the range for magnetic enhancement down from the range of Fe_2O_3 solid solutions stated by Nell and Den Hoed (1997) and Nord et al (1989) quoted in paragraph 2.3.10.4.

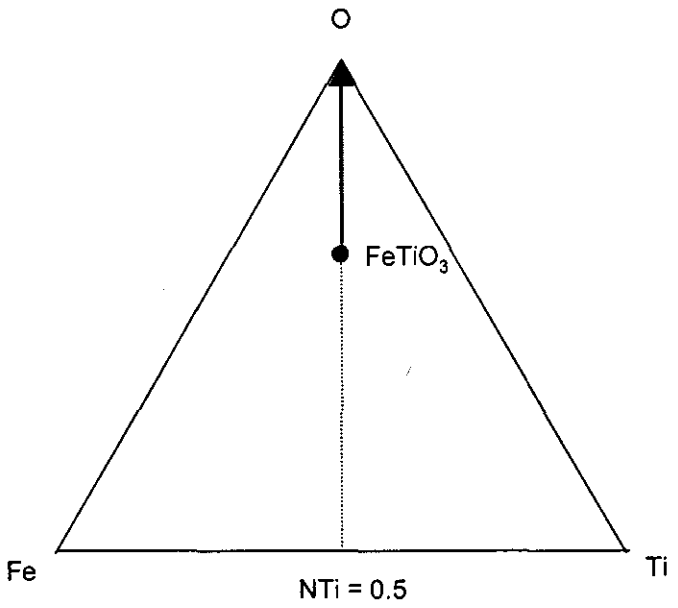

Figure 2.20: Schematic Fe-O-Ti phase diagram indicating the oxidation of ilmenite (mole percentage).

2.11.2 700°C

From the phase diagram at 700°C of Borowiec et al (1981) ilmenite ($FeTiO_3$) will change as follows during oxidation (figure 2.21):

1. TO a mixture containing rutile/anatase (TiO_2) and ilmenite-hematite solid solution (M_2O_3 - with increasing Fe_2O_3 content with increasing oxidation);

2. THEN a mixture containing rutile/anatase (TiO_2), magnetite-Fe_2TiO_4 solid solution (M_3O_4) and ilmenite-hematite solid solution (M_2O_3);
3. THEN a mixture containing rutile/anatase (TiO_2) and pseudobrookite solid solution ($FeTi_2O_5$-Fe_2TiO_5 - with increasing Fe_2TiO_5 content with increasing oxidation).

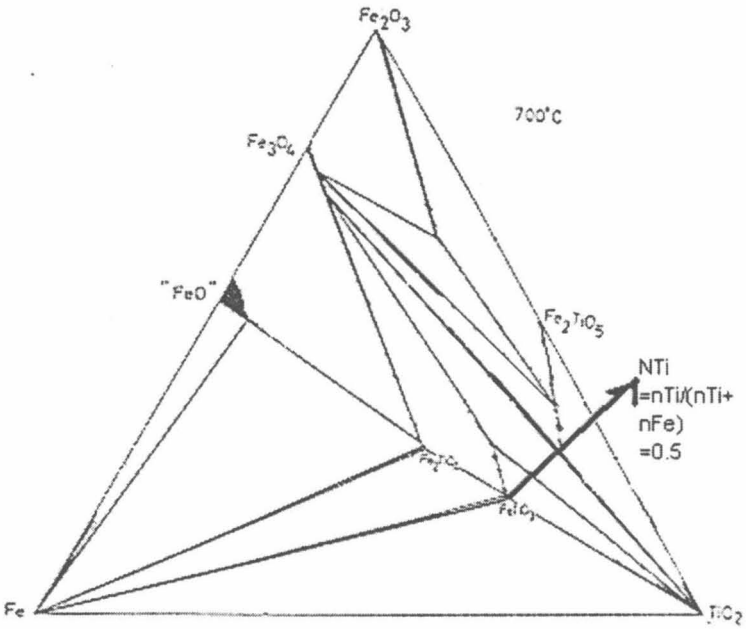

Figure 2.21: Fe-Fe_2O_3-TiO_2 phase diagram at 700°C with components in mole percentages (Borowiec et al 1981). The arrow indicates the path followed during oxidation of $FeTiO_3$.

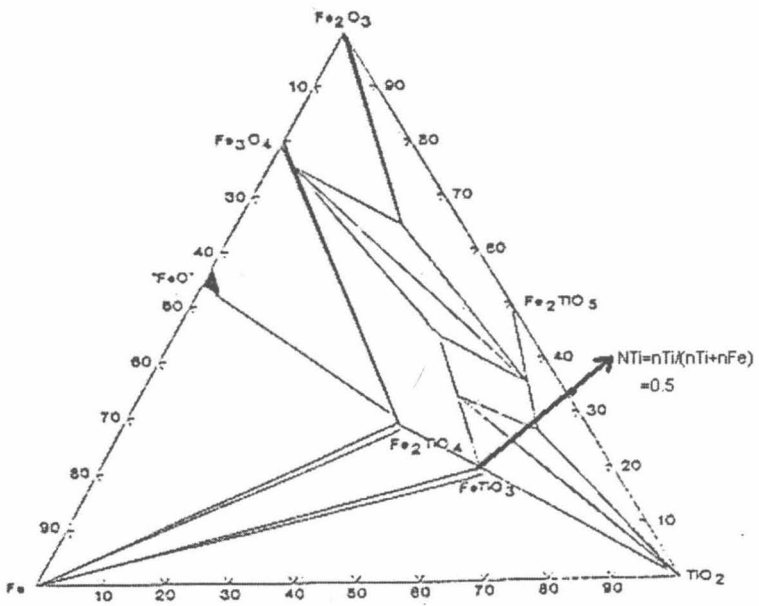

Figure 2.22: Fe-Fe_2O_3-TiO_2 phase diagram at 700°C with components in mole percentages (Gupta et al 1989). The arrow indicates the path followed during oxidation of $FeTiO_3$.

Gupta et al (1989) reviewed the phase diagrams proposed by Borowiec et al (1981). Their experiments confirmed the diagrams at 950°C, but differed considerably at 700°C. From their phase diagram at 700°C ilmenite ($FeTiO_3$) will change (figure 2.22):

4. TO a mixture containing rutile/anatase (TiO_2) and ilmenite-hematite solid solution (M_2O_3 - with increasing Fe_2O_3 content with increasing oxidation);

5. THEN a mixture containing rutile/anatase (TiO_2), pseudobrookite solid solution (M_3O_5) and ilmenite-hematite solid solution (M_2O_3 - fixed at $[Fe_2O_3]_{0.16}[FeTiO_3]_{0.84}$);
6. THEN a mixture containing ilmenite-hematite solid solution (M_2O_3 - with increasing Fe_2O_3 content with increasing oxidation) and pseudobrookite solid solution ($FeTi_2O_5$-Fe_2TiO_5 - with increasing Fe_2TiO_5 content with increasing oxidation) and;
7. THEN a mixture containing rutile/anatase (TiO_2) and pseudobrookite solid solution ($FeTi_2O_5$-Fe_2TiO_5 - with increasing Fe_2TiO_5 content with increasing oxidation).

2.11.3 800°C

Van Dyk (1999 p 77) described what happens at 800°C under equilibrium conditions (from Borowiec et al 1981). Material, with a phase composition close to theoretical ilmenite ($FeTiO_3$), will change during oxidation (figure 2.23):

1. TO a mixture containing rutile/anatase (TiO_2) and ilmenite-hematite solid solution (M_2O_3 - with increasing Fe_2O_3 content with increasing oxidation);
2. THEN a mixture containing rutile/anatase (TiO_2), pseudobrookite solid solution (M_3O_5 fixed at $[FeTi_2O_5]_x[Fe_2TiO_5]_y$) and ilmenite-hematite solid solution (M_2O_3 - fixed at $[Fe_2O_3]_{0.15}[FeTiO_3]_{0.85}$) and;
3. THEN a mixture containing rutile/anatase (TiO_2) and pseudobrookite solid solution ($FeTi_2O_5$-Fe_2TiO_5 - with increasing Fe_2TiO_5 content with increasing oxidation).
4. Evidently, full oxidation of ilmenite will eliminate the hematite-ilmenite solid solution with enhanced magnetic susceptibility. In the next section the equilibrium conditions for this solid solution are estimated.

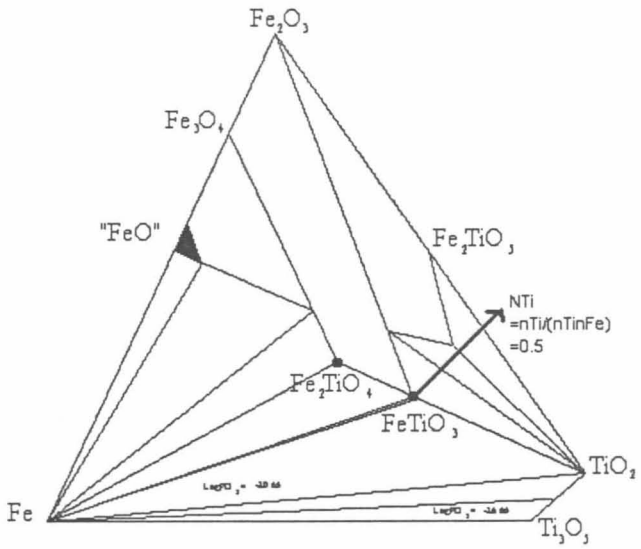

Figure 2.23: Fe-Fe_2O_3-TiO_2 phase diagram at 800° with components as mole percentages (Van Dyk 1999, from Borowiec 1981). The arrow indicates the path followed during oxidation of $FeTiO_3$.

2.11.4 The effect of pO_2 and temperature

The chemical reaction for the oxidation of ilmenite in the TiO_2–M_2O_3 phase field is given as reaction 2-1. With this reaction one can estimate the equilibrium roasting conditions (temperature and pO_2) to obtain 20 to 33 per cent ferric iron (Fe^{3+}) in solid solution in ilmenite. This, as well as the temperature at which the ilmenite is cooled, will result in an ordered R-3-crystal structure (Nell 1999).

When determining the relationship between pO_2 and Fe_2O_3 at a specific temperatures under equilibrium conditions, the following assumptions are made (Nell, 1999):

1. $a_{TiO2}^{Rutile} = 1$, because rutile is virtually pure TiO_2.
2. $X_{Fe2O3}^{ilmenite} + X_{FeTiO3}^{ilmenite} = 1$
3. $\gamma_{FeTiO3}^{ilmenite} = (\gamma_{Fe2O3}^{ilmenite})^{0.5}$ (assumed in the absence of equilibrium data)

The symbols used for the mole fractions and Raoultian activity coefficients are:

- X_x^y = mol fraction x in y
- γ_x^y = activity coefficient of x in y

The resulting relationship is:
$K = e^{-\Delta G^\circ/RT} = (X_{Fe2O3})^{0.5}/((1-X_{Fe2O3})(P_{O2})^{0.25})$

The results at various temperatures are given in the figure 2.24 (thermodynamic data from Kubaschewski et al, 1988-1994).

From the 800°C phase diagram the maximum amount of Fe_2O_3, which can go into solid solution in $FeTiO_3$, is 15-16 per cent. From figure 25 the associated pO_2 is $10^{-12.2}$ atm at 800°C. Borowiec et al (1981) did EMF measurements to determine the oxygen potential for all phase combinations, as a function of temperature. This was for the Fe- Fe_2O_3-TiO_2 system. The pO_2 value that they obtained for M_2O_3-M_3O_5-TiO_2 equilibrium above 780°C is $10^{-11.5}$atm.

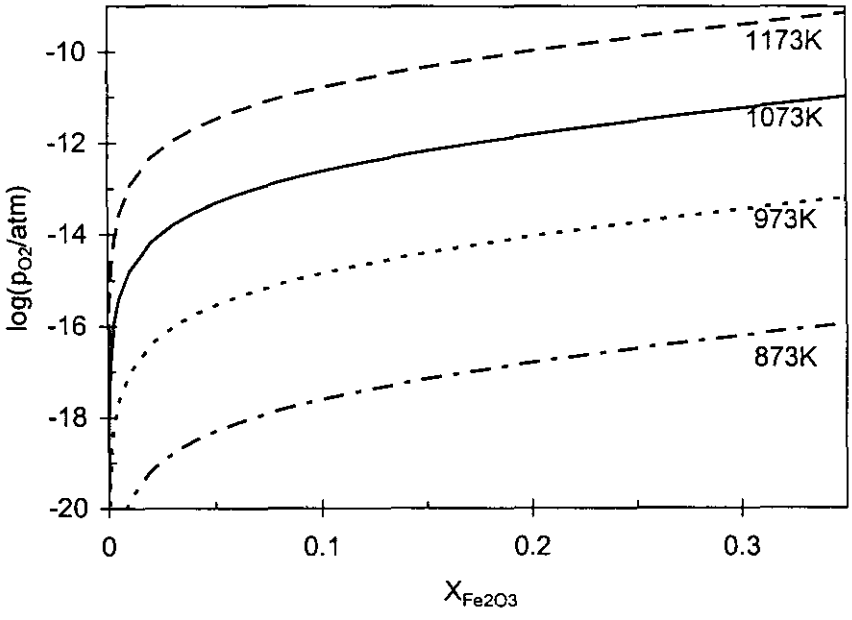

Figure 2.24: Equilibrium oxygen potential as a function of the percentage hematite in solid solution in ilmenite, at various temperatures. Calculated from thermodynamic data from Kubaschewski et al (1988-1994).

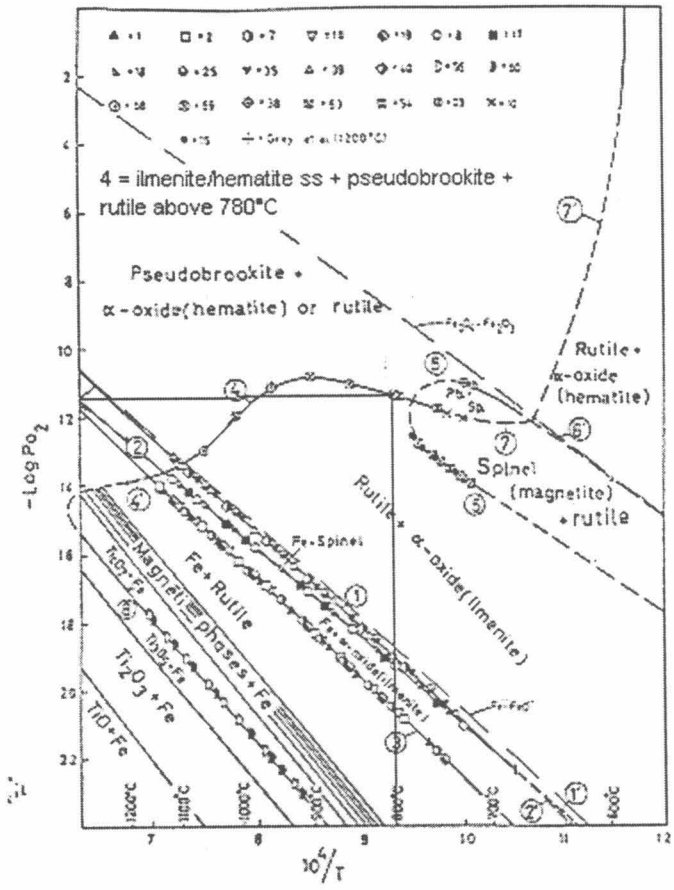

Figure 2.25: Oxygen potential for various phase combinations as a function of temperature, determined from regressional analysis of EMF measurements (Borowiec et al, 1981).

This result correlates fairly well with the results generated from thermodynamic data. It also indicates that at equilibrium conditions the roasting atmosphere need not be very oxidizing to obtain ilmenite with 15 to 16 per cent Fe_2O_3 in solution – figure 2.25.

2.12 Equipment

2.12.1 Laboratory scale equipment

It is concluded from the discussion above that to decrease the Cr_2O_3 content of a crude ilmenite concentrate from 0.3 per cent to 0.1 per cent the following approach was used:

- Authors such as Nell and Den Hoed (1997) exploited the magnetic susceptibility property of both ilmenite and Cr_2O_3 containing spinels;
- They constructed a separability curve for an unroasted concentrate by dividing the concentrate into 10 fractions by adjusting the current settings on a Frantz isodynamic magnetic separator and subjecting each fraction to chemical analysis;
- They roasted samples of crude ilmenite at various roasting conditions and measured the magnetic susceptibility of the roasted material using an inductivity bridge using an alternating current technique;
- They constructed a separability curve for a roasted sample in a fashion similar to that for an unroasted sample.

Therefore the laboratory scale equipment they required were:

- Batch roasting equipment;
- A magnetic separator.

a) Laboratory scale magnetic separators

On laboratory scale equipment Kelly & Spottiswood (1995) mentioned that a Frantz isodynamic separator could be used to construct separability curves based on magnetic susceptibility properties of minerals. Nell and Den Hoed (1997) indeed reported the use thereof in their test work. A Frantz isodynamic separator was also the type of separator used in the present study due its availability at Kumba R&D, where the test work were conducted, and the minimization of forces (other than magnetic forces) applied to a particle in a Frantz separator. The competing forces on particles in any magnetic separator are (Kelly and Spottiswood 1995) gravity, hydrodynamic drag, friction, inertia and centrifugal – in rotating drum separators. When using a Frantz isodynamic magnetic separator to construct separability curves:

- Hydrodynamic drag is negligible because material is tested dry;
- The effect of friction and inertia is minimized because the separator surface is made of polished steel, installed at a slight angle and vibrated;
- No centrifugal forces are present because a rotating drum is not used.

The only forces of importance acting on a particle in a Frantz isodynamic separator are therefore that caused by the applied magnetic field (H) and gravity. If the material is tested dry the magnitude of the gravitational force remains constant.

The Frantz isodynamic separator utilizes specially shaped pole-pieces to produce a force that is almost independent of the distance in a region between pole-pieces. A narrow chute is placed between the pole-pieces and the material to be separated passes down the inclined chute under the influence of gravity. The chute is inclined both parallel and perpendicular to its length so that a component of gravitational force may compete with the magnetic force. Under the influence of gravitational and magnetic forces the grains migrate to one side or the other of the chute, which at one part is divided into two passages by a splitting ridge, which directs the products into two separate containers – figure 2.26 (Svoboda 1987).

Inclination of the chute is measured by the transverse slope θ and the longitudinal slope φ. The pole design is such that changes in the magnetic field exactly balance changes in the field gradient to yield a constant product HdH/dx. In figure 2.26 particles enter the chute at point A. For a paramagnetic particle if the gravity (Fg) and the magnetic (Fm) forces are balanced to cause the paramagnetic particle to move along AB, the particle has a 50 per cent chance of reporting to the magnetic or non-magnetic fraction. The force balance is stated in equation 2.8.

$$Fg = Fm$$

Or

$$mg\sin\theta = \tfrac{1}{2}\mu_0 \kappa V(H)^2$$

Equation 2.8: The force balance in a Frantz magnetic separator with m the particle mass, θ the transverse slope, g the gravitational constant, κ the volume magnetic susceptibility and H the magnetic field strength (Svoboda 1987)

When rewriting equation 2.8 as in equation 2.9, with HdH/dx constant due to the pole design, the action of the separator on a single particle is determined solely by the mass susceptibility of the particle and not on the size or mass of the particle.

$$\sin\theta = \mu_0 \chi H/g.\delta H/\delta x$$

Equation 2.9: Rearranging equation 2.8 with χ the mass or specific magnetic susceptibility (Svoboda 1987)

By calibrating the Frantz separator with chemical compounds with a known magnetic susceptibility, the Frantz can be used to determine the mass susceptibility of specific material fractions – for more details on this method refer to Svoboda (1987).

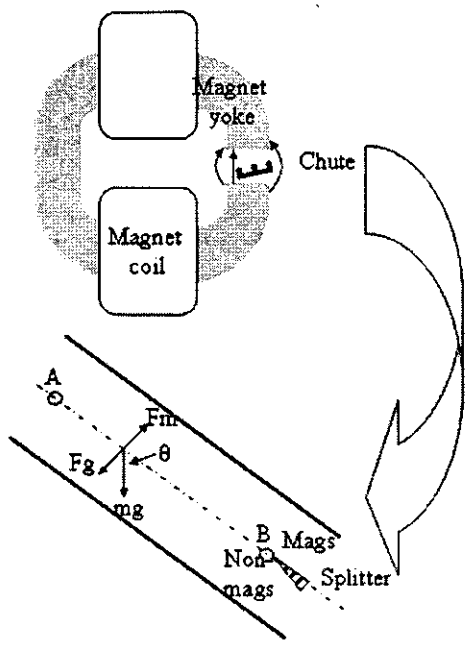

Figure 2.26: Schematic drawing of the Frantz isodynamic separator and the forces acting on a particle in the separator (Svoboda 1987).

Other magnetic separation equipment available on a laboratory scale, but which were not used in this study, include:

- Carpco induced roll magnet;
- Carpco permanent magnet ;
- Davis tube (Svoboda 1987) ;
- Laboratory high-gradient magnetic separators (Svoboda 1987).

b) Laboratory scale roasting equipment

Equipment available for batch roasting include:

- Muffle furnaces;
- Rotating reactors; and
- Fluidised bed reactors.

As I wanted to compare the results of my study to results published in literature (Bergeron and Prest 1974; Nell and Den Hoed 1997), and because of its availability at KUMBA R&D, I decided to utilise a batch fluidised bed reactor.

2.12.2 Full scale magnetic separators

This study does not include a study of the commercially available magnetic separators. What needs to be mentioned here is that two categories of commercially available magnetic separators exist (Kelly and Spottiswood 1995):

- *Low intensity* magnetic separators to be used for the separation of ferromagnetic and paramagnetic minerals with high magnetic susceptibility, from minerals with lower magnetic susceptibilities; and
- *High intensity* magnetic separators to be used for the separation of paramagnetic minerals with lower magnetic susceptibility, from minerals with lower magnetic susceptibilities.

Separation on both low and high intensity machines can be carried out wet or dry. Authors that published papers on the application of various types of magnetic separators include Hopstock (1975), Erasmus (1997), Balderson (1999), Arvidson and Rademeyer (1997), Van der Westhuisen (2001) and Arvidson (2001) to mention but a few.

2.12.3 Full scale roasting equipment

Equipment used for full-scale continuous roasting includes rotary kilns and fluidized bed reactors.

2.13 Findings and conclusions

From this discussion it becomes clear that naturally occurring ilmenite concentrates from South African East Coast deposits contain as much as 0.3 per cent Cr_2O_3 which has to be upgraded to produce smelter grade ilmenite with less than 0.1 per cent Cr_2O_3. If the ilmenite and chromite particles are discrete particles as expected, i.e. no intergrowth between the ilmenite and chromite, the property exploited to achieve this is the difference in magnetic susceptibility of ilmenite and chromite containing minerals. Pure ilmenite is antiferromagnetic, i.e. has a low magnetic susceptibility, but the magnetic susceptibility thereof can be enhanced by obtaining Fe_2O_3 in solid solution and ordering the crystal structure of the solid solution. To ensure that this condition is met the Fe_2O_3 in solid solution should be controlled between 15 per cent and 30 per cent and the material should be slow cooled after roasting. Depending on the state of oxidation of the naturally occurring ilmenite, enhancement of magnetic susceptibility can be obtained by roasting in reducing, in oxidizing or in neutral atmospheres. Roasting conditions to enhance the magnetic susceptibility of ilmenite in South African East Coast deposits are oxidizing roasting conditions. Likewise I expected the magnetic susceptibility of chromite to increase should the Fe_2O_3 content thereof increase. To be able to test the hypotheses I decided to follow a similar test procedure as published by Nell and Den Hoed (1997) and to conduct my roasting tests in conductions published by Bergeron and Prest (1974).

In short: the aim of chapter 2 was to review the current body of knowledge available on ilmenite roasting. The review was organized according to:

- The application of magnetic separation to beneficiate chromite containing ilmenite concentrates in industry;
- Magnetism and the mechanism of changes in magnetic susceptibility of ilmenite;
- The enhancement of the magnetic susceptibility of ilmenite by roasting in various atmospheres, with special emphasis on oxidative roasting; and
- Equipment used in ilmenite roasting and magnetic separation.

I concluded the chapter with a discussion on how I derived my test program from this scholarship review. In chapter 3 this test programme is discussed in more detail.

2.14 Appendix 1: Calculation of the chemical composition of roasted ilmenite based on the findings of Walpole (1991)

From $xFeTiO_3.(1-x)Fe_2O_3$ and Fe^{3+}:Fe^{2+} 1:1 to 1.57:1 (Walpole 1991)

For Fe^{3+}:Fe^{2+} 1:1:
$Fe^{3+}/Fe^{2+} = 2(1-x)/x = (2-2x)x = 1$
Therefore:
$2-2x = x$
$2 = 3x$
$x = 2/3 = 0.67$.....(1)

For Fe^{3+}:Fe^{2+} 1.57:1:
$Fe^{3+}/Fe^{2+} = 2(1-x)/x = (2-2x)x = 1.57$
Therefore:
$2-2x = 1.57x$
$2 = 3.57x$
$x = 2/3.57 = 0.56$.....(2)

To calculate the mole per cent Fe_2O_3 in (1): $0.67FeTiO_3.(0.33)\ Fe_2O_3$
Mole per cent $Fe_2O_3 = 0.33/(0.67+0.33)*100 = 33\%$

To calculate the mole per cent Fe_2O_3 in (2): $0.56FeTiO_3.(0.44)\ Fe_2O_3$
Mole per cent $Fe_2O_3 = 0.44/(0.56+0.44)*100 = 44\%$